Mon. Not. R. Astron. Soc. **000**, 000–000 (0000) Printed 10 June 2014 (MN LATEX style file v2.2)

Evolution of eccentricity and orbital inclination of migrating planets in 2:1 mean motion resonance

Jean Teyssandier[1⋆] and Caroline Terquem[2,1]†
[1] *Institut d'Astrophysique de Paris, UPMC Univ Paris 06, CNRS, UMR7095, 98 bis bd Arago, F-75014, Paris, France*
[2] *Department of Astrophysics, University of Oxford, Keble Road, Oxford OX1 3RH, UK*

10 June 2014

arXiv:1406.2189v1 [astro-ph.EP] 9 Jun 2014

ABSTRACT

We determine, analytically and numerically, the conditions needed for a system of two migrating planets trapped in a 2:1 mean motion resonance to enter an inclination–type resonance. We provide an expression for the asymptotic equilibrium value that the eccentricity $e_{\rm i}$ of the inner planet reaches under the combined effects of migration and eccentricity damping. We also show that, for a ratio q of inner to outer masses below unity, $e_{\rm i}$ has to pass through a value $e_{\rm i,res}$ of order 0.3 for the system to enter an inclination–type resonance. Numerically, we confirm that such a resonance may also be excited at another, larger, value $e_{\rm i,res} \simeq 0.6$, as found by previous authors. A necessary condition for onset of an inclination–type resonance is that the asymptotic equilibrium value of $e_{\rm i}$ is larger than $e_{\rm i,res}$. We find that, for $q \leq 1$, the system cannot enter an inclination–type resonance if the ratio of eccentricity to semimajor axis damping timescales t_e/t_a is smaller than 0.2 . This result still holds if only the eccentricity of the outer planet is damped and $q \lesssim 1$. As the disc/planet interaction is characterized by $t_e/t_a \sim 10^{-2}$, we conclude that excitation of inclination through the type of resonance described here is very unlikely to happen in a system of two planets migrating in a disc.

Key words: celestial mechanics – planetary systems – planetary systems: formation – planetary systems: protoplanetary discs – planets and satellites: general

1 INTRODUCTION

At the time of writing, 98 extrasolar multiple planet systems have been detected by radial velocity surveys and 420 by the *Kepler* mission (Rowe et al. 2014, Lissauer et al. 2014). A significant fraction of these systems contain planet pairs in or near a 2:1 mean motion resonance (Lissauer et al. 2011, Fabrycky et al. 2012, see also Petrovich et al. 2013).

Capture in mean motion resonance is thought to be the result of convergent migration of planets (Snellgrove et al. 2001). Several studies (Lee & Peale 2002, Beaugé, Ferraz–Mello & Michtchenko 2003, Lee 2004, Kley et al. 2005), focussing on the dynamics of the two planets in 2:1 mean motion resonance in the system GJ 876, were published soon after the discovery of this system (Marcy et al. 2001). They assume coplanar orbits and focus on explaining the unusual fact that the orbits of the two planets librate about apsidal alignment in this system (as opposed to anti–alignment in the Io–Europa system). The evolution of planetary systems in mean motion resonance has also been studied with three–dimensional simulations (Thommes & Lissauer 2003, Libert & Tsiganis 2009, Lee & Thommes 2009). It has been found that a system of planets in an eccentricity–type resonance may enter an inclination–type resonance if the eccentricity of the inner planet becomes large enough. In this context, very high orbital inclinations can be reached starting from nearly coplanar configurations.

Studies of resonant inclination excitation are important as this mechanism has been proposed to explain the fact that some extrasolar planets have an orbit which is inclined with respect to the stellar equatorial plane.

Other processes which have been put forward to produce such an inclination include interactions between the planet and

⋆ E-mail: teyssand@iap.fr
† E-mail: caroline.terquem@astro.ox.ac.uk

a companion (Fabrycky & Tremaine 2007, Wu, Murray & Ramsahai 2007, Chatterjee et al. 2008, Naoz et al. 2011, Wu & Lithwick 2011), misalignment of the disc in which the planet forms (Bate, Lodato & Pringle 2010, Batygin 2012, Terquem 2013), tilting of the stellar spin axis due to interaction with the disc (Foucart & Lai 2011, Lai, Foucart & Lin 2011) or dynamical relaxation of a population of planets (Papaloizou & Terquem 2001).

The studies of inclination–type resonances published so far, which are numerical, have mapped to some extent the parameter space and have shown that the onset of resonant inclination excitation depends sensitively on the eccentricity damping timescale and the ratio of the planets' masses.

In this paper, we derive analytically a necessary condition for the onset of inclination–type resonance. The analysis has to be done to second order in eccentricities and inclinations. We also perform numerical simulations to investigate the regime of high eccentricities. We now review eccentricity– and inclination–type resonances before giving an outline of the plan of the paper.

1.1 Eccentricity– and inclination– type resonances

In this paper, we are interested in the case where convergent migration of two planets has led to capture into a 2:1 mean motion resonance. First order eccentricity–type resonance involves only the resonant arguments $2\lambda_o - \lambda_i - \varpi_{i,o}$, where $\lambda_{i,o}$ and $\varpi_{i,o}$ are the mean longitudes and longitudes of pericenters of the inner and outer planets, respectively, and is not associated with a variation of the inclinations (see section 2.2 below). Inclination–type resonance is of second order and involves the resonant arguments $4\lambda_o - 2\lambda_i - 2\Omega_{i,o}$ and $4\lambda_o - 2\lambda_i - \Omega_i - \Omega_o$, where $\Omega_{i,o}$ are the longitudes of ascending nodes of the planets. As shown by Thommes & Lissauer (2003), it requires the eccentricity of the inner planet to reach relatively large values to be excited.

Depending on the eccentricities and masses of the planets, stable eccentricity–type resonances can be (Beaugé, Ferraz–Mello & Michtchenko 2003, Lee 2004):
(i) symmetric with both resonant arguments librating about 0° (and $\varpi_o - \varpi_i$ librating about 0°, i.e. the apsidal lines are aligned and conjunction occurs when the planets are near pericenter),
(ii) anti–symmetric with the resonant arguments librating about 0° and 180°, respectively (and $\varpi_o - \varpi_i$ librating about 180°, i.e. the apsidal lines are anti–aligned and conjunction occurs when one planet is near pericenter and the other near apocenter),
(iii) asymmetric with the resonant arguments librating about angles far from 0° and 180°.

Resonances are stable if the distance between the planets at conjunctions stays large enough. To understand the physics of resonance, let us consider the case of conjunction occurring when the planets are near an apse, i.e. librating about 0° or 180°. In that case, the tangential force exerted by one planet onto the other integrates to zero over an orbit and there is no exchange of angular momentum. The next conjunction therefore occurs at the same longitude. However, if the outer planet is migrating inward (over a timescale much longer than the orbital period), the conjunction occurs slightly away from the stable longitude. In that case, there is a net tangential force which results in the planets exchanging angular momentum in such a way that subsequent conjunctions will be closer to the stable longitude. Therefore, commensurability is maintained and the inner planet is pushed inward (Goldreich 1965, Peale 1976). It can also be shown that during the migration process the radial perturbative force between the planets tends to increase their eccentricities (Lissauer et al. 1984).

If the eccentricities are small, the net tangential force exerted by one planet onto the other is small and therefore the transfer of angular momentum between the two planets is weak. However, in that case, the radial force is much more effective in changing the orientation (causing the regression) of the line of apses and therefore in maintaining the orientation of the apses with the conjunction longitude (Peale 1976, Greenberg 1977). The eccentricity–type resonance therefore exists even for small eccentricities.

For inclination–type resonances, conjunctions librate about the longitude of a node of one planet. There is however no resonance for low inclinations. This is because although the orientation of the lines of nodes can be more easily varied when the inclination is small, the normal perturbative force between the planets, which tends to vary the orientation of the lines of nodes, becomes smaller when the inclination decreases (Greenberg 1977).

1.2 Plan of the paper

In section 2, we develop an analysis, valid to second order in eccentricities and inclinations, of a system of two planets embedded in a disc and in 2:1 mean motion resonance. We give an expression of the disturbing function in section 2.1, write Lagrange's planetary equations in section 2.2 and explain how migration and eccentricity damping are included in section 2.3. We assume that the semimajor axis and the eccentricity of the outer planet are damped by interaction with the disc, and consider both the case where the eccentricity of the inner planet is damped and the case where it is not. In section 2.4, we derive a necessary condition for the onset of inclination–type resonance. We find that, for a ratio q of inner mass to outer mass below unity, the eccentricity of the inner planet has to reach $e_{i,res} \sim 0.3$ for an inclination–type resonance to be excited. This cannot be achieved for $t_{ei}/t_a < 0.2$, where t_{ei} and t_a are the timescales over which the eccentricity of the inner planet

and the semimajor axis of the outer planet are damped. We also find that the onset of the inclination–type resonance requires the eccentricity of the outer planet to reach a critial value $e_{\rm o,res}$. In section 3, we present the results of N–body simulations. We write the equations of motion which are solved in the code in section 3.1 and give the initial setting in section 3.2. In section 3.3, we describe three illustrative cases corresponding to three different values of the eccentricity damping timescale in the case where the eccentricities of both planets are damped over the same timescale t_e. We compare numerical and analytical results in section 3.4, investigate how the onset of inclination–type resonance depends on q and t_e/t_a in section 3.5 and study the influence of varying parameters in section 3.6. In section 3.7, we consider the case where eccentricity damping affects only the outer planet. The effect of inclination damping is discussed in section 3.8. These simulations confirm the analysis and show that there is another, larger, value of $e_{\rm i,res} \simeq 0.6$ (which was found by Thommes & Lissauer 2003). The simulations also show that the onset of inclination–type resonance requires the eccentricity of the outer planet to reach $e_{\rm o,res} \sim 0.2$ when $q \lesssim 1$. The resonant argument ϕ_2 librates about 180° or 0° (while ϕ_1 librates about 0°) depending on whether the system enters an inclination–type resonance with $e_{\rm i,res} \simeq 0.3$ or 0.6, respectively. Finally, in section 4 we summarize and discuss our results.

2 ANALYSIS OF THE RESONANCE

2.1 Disturbing function

We consider two planets of masses $m_{\rm i}$ and $m_{\rm o}$ orbiting a star of mass $m_\star$. The subscripts 'i' and 'o' refer to the inner and outer planets, respectively. The orbital elements $\lambda_{\rm i}$, $a_{\rm i}$, $e_{\rm i}$, $I_{\rm i}$, $\varpi_{\rm i}$ and $\Omega_{\rm i}$ denote the mean longitude, semi–major axis, eccentricity, inclination, longitude of pericenter and longitude of ascending node of the planet of mass $m_{\rm i}$, with same quantities with subscript 'o' for the planet of mass $m_{\rm o}$. We suppose that the two planets are close to or in a 2:1 mean motion commensurability, i.e. the ratio of the mean motions, $n_{\rm i}/n_{\rm o}$, is close or equal to 2. The dynamics is therefore dominated by the resonant and secular terms in the disturbing function, since all the other terms are short–period and average out to zero over the orbital periods.

The perturbing functions for the inner and outer planets can be written under the form (Murray & Dermott 1999):

$$\langle \mathcal{R}_{\rm i} \rangle = \frac{G m_{\rm o}}{a_{\rm o}} \left(\langle \mathcal{R}_{\rm D}^{\rm sec} \rangle + \langle \mathcal{R}_{\rm D}^{\rm res} \rangle + \alpha \langle \mathcal{R}_{\rm E} \rangle \right), \tag{1}$$

$$\langle \mathcal{R}_{\rm o} \rangle = \frac{G m_{\rm i}}{a_{\rm o}} \left(\langle \mathcal{R}_{\rm D}^{\rm sec} \rangle + \langle \mathcal{R}_{\rm D}^{\rm res} \rangle + \frac{1}{\alpha^2} \langle \mathcal{R}_{\rm I} \rangle \right), \tag{2}$$

where G is the constant of gravitation, $\alpha \equiv a_{\rm i}/a_{\rm o}$, $\langle \mathcal{R}_{\rm D}^{\rm sec} \rangle$ and $\langle \mathcal{R}_{\rm D}^{\rm res} \rangle$ are the secular and resonant contributions to the direct part of the disturbing function, respectively, $\langle \mathcal{R}_{\rm E} \rangle$ is the indirect part due to an external perturber and $\langle \mathcal{R}_{\rm I} \rangle$ is the indirect part due to an internal perturber. The brackets indicate that the quantities are time–averaged. Note that there is no secular contribution to $\langle \mathcal{R}_{\rm E} \rangle$ and $\langle \mathcal{R}_{\rm I} \rangle$.

When an expansion of the perturbing function in the orbital elements is carried out, the lowest orders at which eccentricities and inclinations appear are the first and second, respectively, and at second order, there are no terms in which eccentricities and inclinations are coupled. To study the inclination–type resonance, second–order terms in eccentricities need to be included. The expansion of the perturbing function to second order is (Murray & Dermott 1999):

$$\langle \mathcal{R}_{\rm D}^{\rm sec} \rangle = K_1 \left(e_{\rm i}^2 + e_{\rm o}^2 \right) + K_2 e_{\rm i} e_{\rm o} \cos\left(\varpi_{\rm i} - \varpi_{\rm o} \right) + K_3 \left(s_{\rm i}^2 + s_{\rm o}^2 \right) + K_4 s_{\rm i} s_{\rm o} \cos\left(\Omega_{\rm i} - \Omega_{\rm o} \right), \tag{3}$$

$$\begin{aligned} \langle \mathcal{R}_{\rm D}^{\rm res} \rangle = {} & e_{\rm i} f_1 \cos\phi_1 + e_{\rm o} f_2 \cos\phi_2 + e_{\rm i}^2 f_3 \cos\phi_3 + e_{\rm i} e_{\rm o} f_4 \cos\phi_4 + e_{\rm o}^2 f_5 \cos\phi_5 \\ & + s_{\rm i}^2 f_6 \cos\phi_6 + s_{\rm i} s_{\rm o} f_7 \cos\phi_7 + s_{\rm o}^2 f_8 \cos\phi_8, \end{aligned} \tag{4}$$

$$\langle \mathcal{R}_{\rm E} \rangle = -2 e_{\rm o} \cos\phi_2, \tag{5}$$

$$\langle \mathcal{R}_{\rm I} \rangle = -\frac{1}{2} e_{\rm o} \cos\phi_2, \tag{6}$$

where $s_{\rm i,o} = \sin\left(I_{\rm i,o}/2\right)$, and the f_i $(i = 1, \ldots, 8)$ and K_i $(i = 1, \ldots, 4)$ are expressed in term of the Laplace coefficients and

α. Their expression is given in Appendix A. The resonant angles ϕ_i ($i = 1, \ldots, 8$) are defined by:

$$\phi_1 = 2\lambda_\mathrm{o} - \lambda_\mathrm{i} - \varpi_\mathrm{i}, \tag{7}$$
$$\phi_2 = 2\lambda_\mathrm{o} - \lambda_\mathrm{i} - \varpi_\mathrm{o}, \tag{8}$$
$$\phi_3 = 4\lambda_\mathrm{o} - 2\lambda_\mathrm{i} - 2\varpi_\mathrm{i}, \tag{9}$$
$$\phi_4 = 4\lambda_\mathrm{o} - 2\lambda_\mathrm{i} - \varpi_\mathrm{o} - \varpi_\mathrm{i}, \tag{10}$$
$$\phi_5 = 4\lambda_\mathrm{o} - 2\lambda_\mathrm{i} - 2\varpi_\mathrm{o}, \tag{11}$$
$$\phi_6 = 4\lambda_\mathrm{o} - 2\lambda_\mathrm{i} - 2\Omega_\mathrm{i}, \tag{12}$$
$$\phi_7 = 4\lambda_\mathrm{o} - 2\lambda_\mathrm{i} - \Omega_\mathrm{i} - \Omega_\mathrm{o}, \tag{13}$$
$$\phi_8 = 4\lambda_\mathrm{o} - 2\lambda_\mathrm{i} - 2\Omega_\mathrm{o}. \tag{14}$$

2.2 Lagrange's planetary equations

When the perturbing function is expanded to second order in the eccentricities and inclinations, Lagrange equations can be written as follows:

$$\frac{da_\beta}{dt} = \frac{2}{n_\beta a_\beta}\frac{\partial \langle \mathcal{R}_\beta \rangle}{\partial \lambda_\beta}, \tag{15}$$
$$\frac{de_\beta}{dt} = \frac{-1}{n_\beta a_\beta^2 e_\beta}\frac{\partial \langle \mathcal{R}_\beta \rangle}{\partial \varpi_\beta}, \tag{16}$$
$$\frac{d\varpi_\beta}{dt} = \frac{1}{n_\beta a_\beta^2 e_\beta}\frac{\partial \langle \mathcal{R}_\beta \rangle}{\partial e_\beta}, \tag{17}$$
$$\frac{d\lambda_\beta}{dt} = n_\beta + \frac{1}{n_\beta a_\beta^2}\left(-2a_\beta\frac{\partial \langle \mathcal{R}_\beta \rangle}{\partial a_\beta} + \frac{e_\beta}{2}\frac{\partial \langle \mathcal{R}_\beta \rangle}{\partial e_\beta} + \tan\frac{I_\beta}{2}\frac{\partial \langle \mathcal{R}_\beta \rangle}{\partial I_\beta}\right), \tag{18}$$
$$\frac{d\Omega_\beta}{dt} = \frac{1}{n_\beta a_\beta^2 \sin I_\beta}\frac{\partial \langle \mathcal{R}_\beta \rangle}{\partial I_\beta}, \tag{19}$$
$$\frac{dI_\beta}{dt} = \frac{-1}{n_\beta a_\beta^2 \sin I_\beta}\frac{\partial \langle \mathcal{R}_\beta \rangle}{\partial \Omega_\beta}, \tag{20}$$

where $\beta = \mathrm{i}, \mathrm{o}$. In equation (18), the derivative with respect to a_β has to be carried out by ignoring the fact that the angles ϕ_i ($i = 1, \ldots, 8$) depend on a_β through λ_i and λ_o (Roy 1978). We define a timescale T such that:

$$T = n_{\mathrm{o}0}^{-1}\,\frac{m_\star}{m_\mathrm{i}}, \tag{21}$$

where the subscript '0' denotes initial value. We consider planets with masses $m_{\mathrm{i,o}} \ll m_\star$, so that the mean motions are approximated by $n_{\mathrm{i,o}} = \left(Gm_\star/a_{\mathrm{i,o}}^3\right)^{1/2}$.

Using the expression of the perturbing function given by equations (1)–(6), we can rewrite Lagrange equations (15)–(20) in the following dimensionless form:

$$\frac{da_\mathrm{i}}{d\tau} = \mathcal{C}_\mathrm{i} 2a_\mathrm{i} \left[e_\mathrm{i} F_1 + e_\mathrm{o} F_2 - e_\mathrm{o} 2\alpha \sin\phi_2 + F_3 + \mathcal{O}(3) \right], \tag{22}$$

$$\frac{da_\mathrm{o}}{d\tau} = \mathcal{C}_\mathrm{o}(-4a_\mathrm{o}) \left[e_\mathrm{i} F_1 + e_\mathrm{o} F_2 - \frac{e_\mathrm{o}}{2\alpha^2} \sin\phi_2 + F_3 + \mathcal{O}(3) \right], \tag{23}$$

$$\frac{de_\mathrm{i}}{d\tau} = \mathcal{C}_\mathrm{i} \left[-F_1 + \mathcal{O}(2) \right], \tag{24}$$

$$\frac{de_\mathrm{o}}{d\tau} = \mathcal{C}_\mathrm{o} \left[-F_2 + \frac{1}{2\alpha^2} \sin\phi_2 + \mathcal{O}(2) \right], \tag{25}$$

$$\frac{d\varpi_\mathrm{i}}{d\tau} = \mathcal{C}_\mathrm{i} \left[\frac{1}{e_\mathrm{i}} f_1 \cos\phi_1 + 2f_3 \cos\phi_3 + \frac{e_\mathrm{o}}{e_\mathrm{i}} f_4 \cos\phi_4 + 2K_1 + K_2 \frac{e_\mathrm{o}}{e_\mathrm{i}} \cos(\varpi_\mathrm{i} - \varpi_\mathrm{o}) + \mathcal{O}(1) \right], \tag{26}$$

$$\frac{d\varpi_\mathrm{o}}{d\tau} = \mathcal{C}_\mathrm{o} \left[\frac{1}{e_\mathrm{o}} \left(f_2 - \frac{1}{2\alpha^2} \right) \cos\phi_2 + \frac{e_\mathrm{i}}{e_\mathrm{o}} f_4 \cos\phi_4 + 2f_5 \cos\phi_5 + 2K_1 + K_2 \frac{e_\mathrm{i}}{e_\mathrm{o}} \cos(\varpi_\mathrm{i} - \varpi_\mathrm{o}) + \mathcal{O}(1) \right], \tag{27}$$

$$\frac{d\lambda_\mathrm{i}}{d\tau} = \mathcal{C}_\mathrm{i} \left[\frac{1}{\alpha} \frac{m_\star}{m_\mathrm{o}} + \frac{1}{2} e_\mathrm{i} f_1 \cos\phi_1 + 4\alpha e_\mathrm{o} \cos\phi_2 - \Delta + \mathcal{O}(2) \right], \tag{28}$$

$$\frac{d\lambda_\mathrm{o}}{d\tau} = \mathcal{C}_\mathrm{o} \left[\frac{m_\star}{m_\mathrm{i}} + 2e_\mathrm{i} f_1 \cos\phi_1 + \frac{1}{2} e_\mathrm{o} \left(5f_2 + \frac{3}{2\alpha^2} \right) \cos\phi_2 + \Delta + \mathcal{O}(2) \right], \tag{29}$$

$$\frac{d\Omega_\mathrm{i}}{d\tau} = \frac{\mathcal{C}_\mathrm{i}}{2} \left[K_3 + \frac{1}{2} \frac{s_\mathrm{o}}{s_\mathrm{i}} \left(K_4 \cos(\Omega_\mathrm{i} - \Omega_\mathrm{o}) + f_7 \cos\phi_7 \right) + f_6 \cos\phi_6 + \mathcal{O}(1) \right], \tag{30}$$

$$\frac{d\Omega_\mathrm{o}}{d\tau} = \frac{\mathcal{C}_\mathrm{o}}{2} \left[K_3 + \frac{1}{2} \frac{s_\mathrm{i}}{s_\mathrm{o}} \left(K_4 \cos(\Omega_\mathrm{i} - \Omega_\mathrm{o}) + f_7 \cos\phi_7 \right) + f_8 \cos\phi_8 + \mathcal{O}(1) \right], \tag{31}$$

$$\frac{dI_\mathrm{i}}{d\tau} = \mathcal{C}_\mathrm{i} \left[\frac{1}{2} \frac{s_\mathrm{o}}{c_\mathrm{i}} \left(K_4 \sin(\Omega_\mathrm{i} - \Omega_\mathrm{o}) - f_7 \sin\phi_7 \right) - \frac{s_\mathrm{i}}{c_\mathrm{i}} f_6 \sin\phi_6 + \mathcal{O}(2) \right], \tag{32}$$

$$\frac{dI_\mathrm{o}}{d\tau} = \mathcal{C}_\mathrm{o} \left[-\frac{1}{2} \frac{s_\mathrm{i}}{c_\mathrm{o}} \left(K_4 \sin(\Omega_\mathrm{i} - \Omega_\mathrm{o}) + f_7 \sin\phi_7 \right) - \frac{s_\mathrm{o}}{c_\mathrm{o}} f_8 \sin\phi_8 + \mathcal{O}(2) \right], \tag{33}$$

where $\tau = t/T$, $c_\mathrm{i,o} = \cos(I_\mathrm{i,o}/2)$, $\mathcal{C}_\mathrm{i} = (a_\mathrm{o0}/a_\mathrm{o})^{3/2} m_\mathrm{o}/(m_\mathrm{i}\sqrt{\alpha})$, $\mathcal{C}_\mathrm{o} = (a_\mathrm{o0}/a_\mathrm{o})^{3/2}$,

$$F_1 = f_1 \sin\phi_1 + 2e_\mathrm{i} f_3 \sin\phi_3 + e_\mathrm{o} f_4 \sin\phi_4 - K_2 e_\mathrm{o} \sin(\varpi_\mathrm{i} - \varpi_\mathrm{o}), \tag{34}$$

$$F_2 = f_2 \sin\phi_2 + 2e_\mathrm{o} f_5 \sin\phi_5 + e_\mathrm{i} f_4 \sin\phi_4 + K_2 e_\mathrm{i} \sin(\varpi_\mathrm{i} - \varpi_\mathrm{o}), \tag{35}$$

$$F_3 = 2s_\mathrm{i}^2 f_6 \sin\phi_6 + 2s_\mathrm{i} s_\mathrm{o} f_7 \sin\phi_7 + 2s_\mathrm{o}^2 f_8 \sin\phi_8 \tag{36}$$

and:

$$\Delta = 2\alpha \left(e_\mathrm{i} \frac{\partial f_1}{\partial \alpha} \cos\phi_1 + e_\mathrm{o} \frac{\partial f_2}{\partial \alpha} \cos\phi_2 \right). \tag{37}$$

Note that, with a perturbing function expanded to second order in eccentricities and inclinations, the rate of change of $\varpi_\mathrm{i,o}$ and $\Omega_\mathrm{i,o}$ can be obtained only to zeroth order in eccentricities and inclinations.

The only orbital elements which are relevant when the orbits are coplanar are $a_\mathrm{i,o}$, $e_\mathrm{i,o}$, $\varpi_\mathrm{i,o}$ and $\lambda_\mathrm{i,o}$. At the order at which the above equations are valid, we note that their evolution is decoupled from that of $\Omega_\mathrm{i,o}$ and $I_\mathrm{i,o}$. Similarly, when the semimajor axes do not vary significantly, the variations of $\Omega_\mathrm{i,o}$ and $I_\mathrm{i,o}$ are decoupled from that of the other orbital elements.

2.3 Modelling of migration and eccentricity damping

We are interested in the case where the two planets capture each other in a mean motion resonance, which happens for instance if the outer planet migrates inward due to its interaction with the disc at least as fast as the inner planet. To model this, we artificially decrease the semimajor axis of the outer planet by adding a damping term $-a_\mathrm{o}/\tau_a$ on the right–hand side of equation (23), where τ_a is the (dimensionless) migration timescale that can be freely specified. In principle, due to its interaction with the disc, the inner planet also migrates independently of the outer one. For simplicity, this is not taken into account here. It would not change the results presented in this paper as long as the inner planet were not migrating faster than the outer one. In this context, the timescale τ_a can be thought of as the timescale over which the outer planet migrates with respect to the inner one. Note that a diminution of a_i, although not being added artificially, will be induced by that of a_o (see below).

Interaction with the disc also leads to damping of the planets eccentricities. This is taken into account by adding a damping term $-e_\mathrm{i}/\tau_{ei}$ and $-e_\mathrm{o}/\tau_{eo}$ on the right–hand side of equations (24) and (25), respectively, where τ_{ei} and τ_{eo} are the (dimensionless) eccentricity damping timescales. Eccentricity damping does in turn contribute to the damping of the semimajor axis by a term $-2a_{\mathrm{i,o}}e_{\mathrm{i,o}}^2/\tau_{\mathrm{ei,o}}$ (see appendix B).

With migration and eccentricity damping taken into account, equations (22)–(25) become:

$$\frac{da_\mathrm{i}}{d\tau} = \mathcal{C}_\mathrm{i} 2a_\mathrm{i}\left[e_\mathrm{i}F_1 + e_\mathrm{o}F_2 - e_\mathrm{o}2\alpha\sin\phi_2 + F_3 + \mathcal{O}(3)\right] - \frac{2a_\mathrm{i}e_\mathrm{i}^2}{\tau_{ei}}, \tag{38}$$

$$\frac{da_\mathrm{o}}{d\tau} = \mathcal{C}_\mathrm{o}(-4a_\mathrm{o})\left[e_\mathrm{i}F_1 + e_\mathrm{o}F_2 - \frac{e_\mathrm{o}}{2\alpha^2}\sin\phi_2 + F_3 + \mathcal{O}(3)\right] - \frac{a_\mathrm{o}}{\tau_a} - \frac{2a_\mathrm{o}e_\mathrm{o}^2}{\tau_{eo}}, \tag{39}$$

$$\frac{de_\mathrm{i}}{d\tau} = \mathcal{C}_\mathrm{i}\left[-F_1 + \mathcal{O}(2)\right] - \frac{e_\mathrm{i}}{\tau_{ei}}, \tag{40}$$

$$\frac{de_\mathrm{o}}{d\tau} = \mathcal{C}_\mathrm{o}\left[-F_2 + \frac{1}{2\alpha^2}\sin\phi_2 + \mathcal{O}(2)\right] - \frac{e_\mathrm{o}}{\tau_{eo}}. \tag{41}$$

In this paper, we will consider either the case $\tau_{ei} = \tau_{eo}$ or the case of infinite τ_{ei} (no damping on the inner planet) and finite τ_{eo}. Inclination damping has not been included, as it is not relevant here (see section 3.8).

2.4 Necessary condition for the onset of inclination–type resonance

In this section, we derive a necessary condition for a pair of planets in 2:1 mean motion resonance to enter an inclination–type resonance. We assume that the planets have captured each other in an exact resonance, so that $\alpha \equiv a_\mathrm{i}/a_\mathrm{o} = 2^{-2/3}$ remains constant in time. In that case, it is useful to note that $2\alpha = 1/(2\alpha^2)$. We also define the mass ratio $q \equiv m_\mathrm{i}/m_\mathrm{o}$.

In this context, equations (38) and (39) can be combined to give:

$$\frac{2}{a_\mathrm{i}}\frac{da_\mathrm{i}}{d\tau} + \frac{1}{q\sqrt{\alpha}}\frac{1}{a_\mathrm{o}}\frac{da_\mathrm{o}}{d\tau} = -\frac{1}{q\sqrt{\alpha}\tau_a} - 4\frac{e_\mathrm{i}^2}{\tau_{ei}} - \frac{2}{q\sqrt{\alpha}}\frac{e_\mathrm{o}^2}{\tau_{eo}}. \tag{42}$$

Using $\alpha = a_\mathrm{i}/a_\mathrm{o}$, we obtain the following differential equation for a_i and a_o:

$$\left(1 + 2q\sqrt{\alpha}\right)\frac{1}{a_\mathrm{i,o}}\frac{da_\mathrm{i,o}}{d\tau} = -\frac{1}{\tau_a} - 4q\sqrt{\alpha}\frac{e_\mathrm{i}^2}{\tau_{ei}} - 2\frac{e_\mathrm{o}^2}{\tau_{eo}}. \tag{43}$$

To first order in eccentricities, the solutions are:

$$a_\mathrm{i,o}(\tau) = a_\mathrm{i0,o0}\; e^{-\tau/\left[(1+2q\sqrt{\alpha})\tau_a\right]}. \tag{44}$$

This shows that, when $q = 0$, i.e., when the inner planet is treated as a test particle, both planets migrate at a rate τ_a. When q is nonzero, the migration is slightly slowed down by the mutual interaction between the two planets.

2.4.1 Eccentricity–type resonance

As a first step, we calculate the equilibrium values reached by the eccentricities under the combined effects of migration and eccentricity damping when the system is in an eccentricity–type resonance with zero inclinations.

Equations (40) and (41) can be combined to give:

$$e_\mathrm{i}\frac{de_\mathrm{i}}{d\tau} + \frac{e_\mathrm{i}^2}{\tau_{ei}} + \frac{1}{q\sqrt{\alpha}}\left(e_\mathrm{o}\frac{de_\mathrm{o}}{d\tau} + \frac{e_\mathrm{o}^2}{\tau_{eo}}\right) = -\mathcal{C}_\mathrm{i}\left[e_\mathrm{i}F_1 + e_\mathrm{o}F_2 - \frac{e_\mathrm{o}}{2\alpha^2}\sin\phi_2 + \mathcal{O}(3)\right] \tag{45}$$

When the inclinations are zero, $F_3 = 0$. Using equations (39) and (43), we can then rewrite equation (45) under the form:

$$\frac{\mathrm{d}e_\mathrm{i}^2}{\mathrm{d}\tau} + \frac{1+q\sqrt{\alpha}}{1+2q\sqrt{\alpha}}\frac{4e_\mathrm{i}^2}{\tau_{ei}} + \frac{1}{q\sqrt{\alpha}}\left[\frac{\mathrm{d}e_\mathrm{o}^2}{\mathrm{d}\tau} + \frac{1+q\sqrt{\alpha}}{1+2q\sqrt{\alpha}}\frac{2e_\mathrm{o}^2}{\tau_{eo}}\right] = \frac{1}{\tau_a(1+2q\sqrt{\alpha})}. \tag{46}$$

When $q \to 0$, e_o has to satisfy $de_\mathrm{o}^2/d\tau + 2e_\mathrm{o}^2/\tau_{eo} = 0$, which means that e_o is damped to zero whereas, in this limit, e_i reaches the equilibrium value $[\tau_{ei}/(4\tau_a)]^{1/2}$.

2.4.1.1 Finite values of τ_{ei} and τ_{eo} : When the eccentricities of both planets are damped and $q \leq 1$, i.e. the outer planet is at least a massive as the inner one, we expect the eccentricity of the outer planet to grow less than that of the inner planet. We therefore neglect the terms involving e_o in equation (46), which then leads to the following equilibrium value (corresponding to $\tau \gg \tau_{ei}$) for e_i:

$$e_{\rm i,eq} = \frac{1}{2}\left(\frac{\tau_{ei}/\tau_a}{1+q\sqrt{\alpha}}\right)^{1/2}. \quad (47)$$

In figure 1, we plot $e_{\rm i,eq}$ as a function of q for $\tau_{ei}/\tau_a = 1$, 0.2 and 0.1. The numerical simulations presented in the next section confirm that neglecting $e_{\rm o}$ in equation (46) is a valid approximation for the parameters of interest in this paper. The numerical values found for $e_{\rm i,eq}$ also agree very well with that given by equation (47), as indicated in Figure 6.

2.4.1.2 Finite value of τ_{eo} and $\tau_{ei} \to \infty$: In some conditions that will be discussed in section 3.7, damping due to tidal interaction with the disc acts only on the eccentricity of the outer planet, not on that of the inner planet. In that case, as the planets are in resonance, $e_{\rm i}$ still reaches an equilibrium value. This is shown by equation (24) in which $F_1 = 0$ when the resonant angles librate about 0° or 180°. By substituting $de_{\rm i}^2/d\tau = 0$ and $\tau_{ei} \to \infty$ in equation (46), we obtain the following equilibrium value (corresponding to $\tau \gg \tau_{eo}$) for $e_{\rm o}$:

$$e_{\rm o,eq} = \left[\frac{q\sqrt{\alpha}\,\tau_{eo}/\tau_a}{2\,(1+q\sqrt{\alpha})}\right]^{1/2}. \quad (48)$$

In figure 2, we plot $e_{\rm o,eq}$ as a function of q for $\tau_{eo}/\tau_a = 0.2$, 0.05 and 0.01. The numerical values found for $e_{\rm o,eq}$ agree very well with that given by equation (48), as indicated in Figure 10.

2.4.2 Inclination–type resonance

We now calculate the values $e_{\rm i,res}$ and $e_{\rm o,res}$ that $e_{\rm i}$ and $e_{\rm o}$, respectively, have to reach for the inclinations to start growing. A necessary condition for the system to enter an inclination–type resonance when both τ_{ei} and τ_{eo} are finite is $e_{\rm i,res} < e_{\rm i,eq}$, where $e_{\rm i,eq}$ is given by equation (47). When $\tau_{ei} \to \infty$, a necessary condition is $e_{\rm o,res} < e_{\rm o,eq}$, where $e_{\rm o,eq}$ is given by equation (48).

Inclination–type resonance can be reached only after an eccentricity–type resonance has been established (Thommes & Lissauer 2003) and therefore all the resonant angles librate about some values. Due to eccentricity damping, libration of the resonant angles is actually offset from a fixed value (generally 0° or 180°) by a term on the order of $e_{\rm i}/\tau_{ei}$ or $e_{\rm o}/\tau_{eo}$ (Goldreich & Schlichting 2014). Because of the $1/\tau_{ei}$ or $1/\tau_{eo}$ factor, this term is much smaller than those retained in the analysis here, so that we will ignore it. Therefore the time–derivative of the resonant angles is close to zero. Equations (7), (8), (12) and (14) then yield:

$$\frac{{\rm d}\varpi_{\rm i}}{{\rm d}\tau} = \frac{{\rm d}\varpi_{\rm o}}{{\rm d}\tau} = \frac{{\rm d}\Omega_{\rm i}}{{\rm d}\tau} = \frac{{\rm d}\Omega_{\rm o}}{{\rm d}\tau}, \quad (49)$$

i.e., the nodes and pericenters all precess at the same rate. In the inclination–type resonance we consider here, as shown in the numerical simulations presented below, the resonant angles ϕ_6, ϕ_7 and ϕ_8 librate about 180°, 0° and 180°, respectively, and $\Omega_{\rm i} - \Omega_{\rm o}$ librates about 180°, in agreement with Thommes & Lissauer (2003). In the analysis that follows, we therefore use $\phi_7 = 0°$, $\phi_6 = 180°$, $\phi_8 = 180°$ and $\Omega_{\rm i} - \Omega_{\rm o} = 180°$.

We first write $d\Omega_{\rm i}/d\tau = d\Omega_{\rm o}/d\tau$ by equating equations (30) and (31). This leads to an algebraic equation for $s_{\rm i}/s_{\rm o}$. Using the fact that $f_6 = f_8$ and $K_3 - f_8 = (-K_4 + f_7)/2$ (see appendix A), we can write the solution of this equation as:

$$\frac{s_{\rm o}}{s_{\rm i}} = q\sqrt{\alpha}. \quad (50)$$

For values of q less than unity, the inclination of the inner planet is more easily excited than that of the outer planet. Note that the ratio of the inclinations does not depend on τ_a nor τ_{ei} or τ_{eo}.

We now write $d\varpi_{\rm o}/d\tau = d\Omega_{\rm o}/d\tau$ by equating equations (27) and (31) and $d\varpi_{\rm i}/d\tau = d\Omega_{\rm i}/d\tau$ by equating equations (26) and (30). In the resulting set of equations, we replace $s_{\rm i}/s_{\rm o}$ by the value found above. This set of two equations can now be solved to calculate $e_{\rm i,res}$ and $e_{\rm o,res}$, which are the values of $e_{\rm i}$ and $e_{\rm o}$, respectively, when the inclination–type resonance is reached. This calculation requires the knowledge of ϕ_1 and ϕ_2 at the time when the inclination–type resonance is triggered. For two planets in 2:1 mean motion resonance, it has been found (e.g. Lee & Peale 2002) that, in general, $(\phi_1, \phi_2) = (0°, 180°)$ or $(0°, 0°)$, depending on whether the eccentricities are small or large, respectively ('large' meaning that second order terms in the eccentricities are not negligible). Fixing $\phi_1 = 0°$ and $\cos^2\phi_2 = 1$, we obtain:

$$e_{\rm i,res} = \frac{-f_1\Delta_3 + \left(f_2 - \frac{1}{2\alpha^2}\right)(f_4 + K_2)}{-(f_4+K_2)^2 + \Delta_3\Delta_4}, \quad (51)$$

$$e_{\rm o,res} = \frac{f_1\,(f_4+K_2) - \Delta_4\left(f_2 - \frac{1}{2\alpha^2}\right)}{\Delta_3\Delta_4 - (f_4+K_2)^2}\cos\phi_2, \quad (52)$$

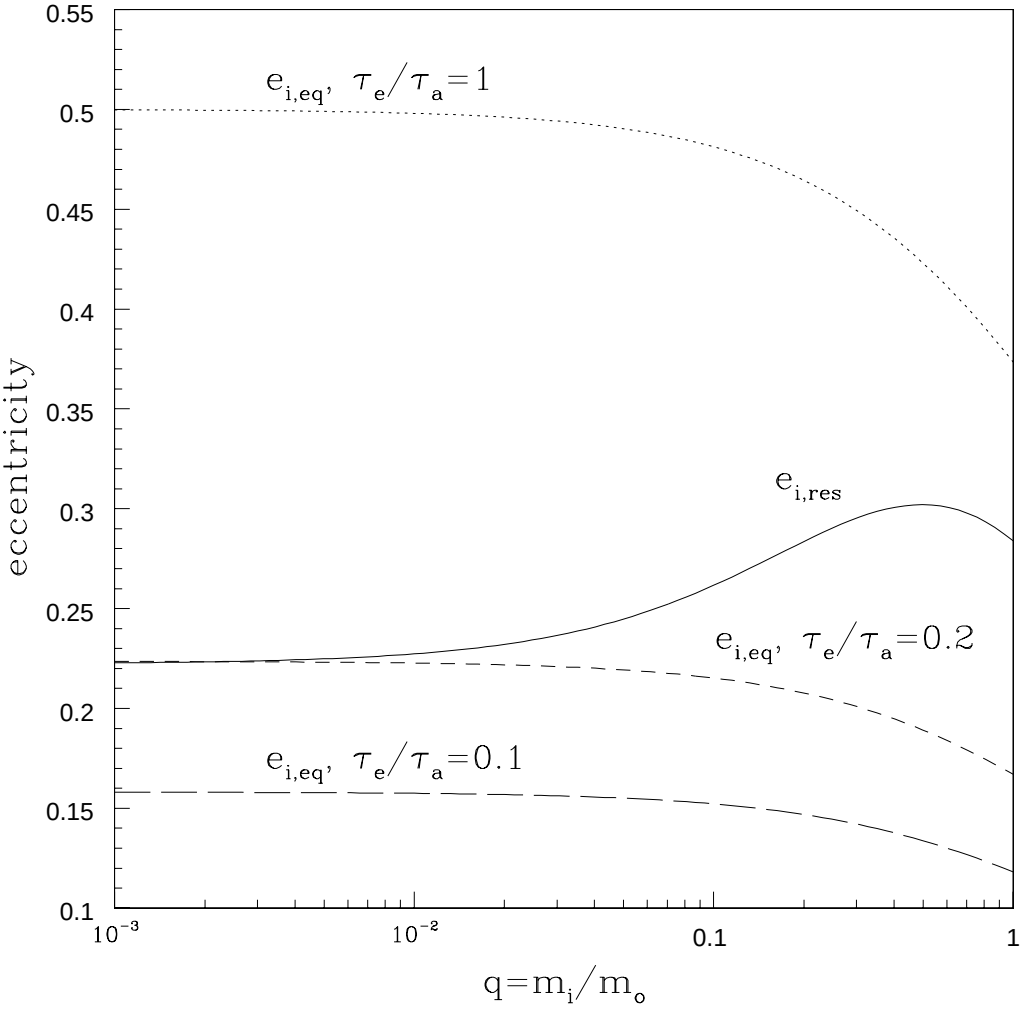

Figure 1. *Solid line:* Eccentricity $e_{\rm i,res}$ of the inner planet when the system enters an inclination–type resonance *versus* q in logarithmic scale. This curve corresponds to equation (51) with $\cos^2\phi_2 = 1$. Also shown is the equilibrium eccentricity for $\tau_{ei}/\tau_a = 0.1$ (*long dashed line*), $\tau_{ei}/\tau_a = 0.2$ (*short dashed line*) and $\tau_{ei}/\tau_a = 1$ (*dotted line*). These curves correspond to equation (47). The system cannot enter an inclination–type resonance when $\tau_{ei}/\tau_a < 0.2$.

where we have defined $\Delta_1 = K_3 + q\sqrt{\alpha}(f_7 - K_4)/2 - f_6$, $\Delta_2 = K_3 + (f_7 - K_4)/(2q\sqrt{\alpha}) - f_8$, $\Delta_3 = 2f_5 + 2K_1 - \Delta_2/2$ and $\Delta_4 = 2f_3 + 2K_1 - \Delta_1/2$.

We note that $e_{\rm i,res}$ and $e_{\rm o,res}$ do not depend on the damping timescales. When $q \to 0$, equations (51) and (52) give $e_{\rm i,res} = f_1/\left[(K_3 - f_6)/2 - 2(f_3 + K_1)\right] \simeq 0.22$ and $e_{\rm o,res} = 0$, respectively.

Equation (52) gives a positive value of the eccentricity for $\phi_2 = 0^\circ$ but a negative value for $\phi_2 = 180^\circ$. When ϕ_2 evolves from libration about 0° to libration about 180°, the apsidal lines evolve from being aligned to being anti–aligned, i.e. the pericentre of the outer orbit is changed to apocentre. In that case, for the equation of the outer ellipse which was used in deriving Lagrange's equations to be preserved, $e_{\rm o}$ should be changed to $-e_{\rm o}$. The value of $e_{\rm o}$ corresponding to $\phi_2 = 180^\circ$ is therefore the opposite as that given by equation (52).

In figure 1, we plot the eccentricity $e_{\rm i,res}$ given by equation (51) as a function of q. For q varying between 0.1 and 1, we see that $e_{\rm i,res} \simeq 0.3$. The eccentricity $e_{\rm o,res}$ given by equation (52) is shown in figure 2. We see that $e_{\rm o,res}$ varies much more with q than $e_{\rm i,res}$.

The numerical results presented in the next section show that there are two regimes in which the system may enter an inclination–type resonance: (i) a *small eccentricity* regime, which is described by the analysis above (although the value of $e_{\rm o,res}$ found numerically is about twice as large as that found analytically), and (ii) a *large eccentricity* regime, in which inclination–type resonance is obtained for $e_{\rm i,res} \simeq 0.6$ and $e_{\rm o,res} \simeq 0.2$ for $q \lesssim 1$. The large eccentricity regime cannot be

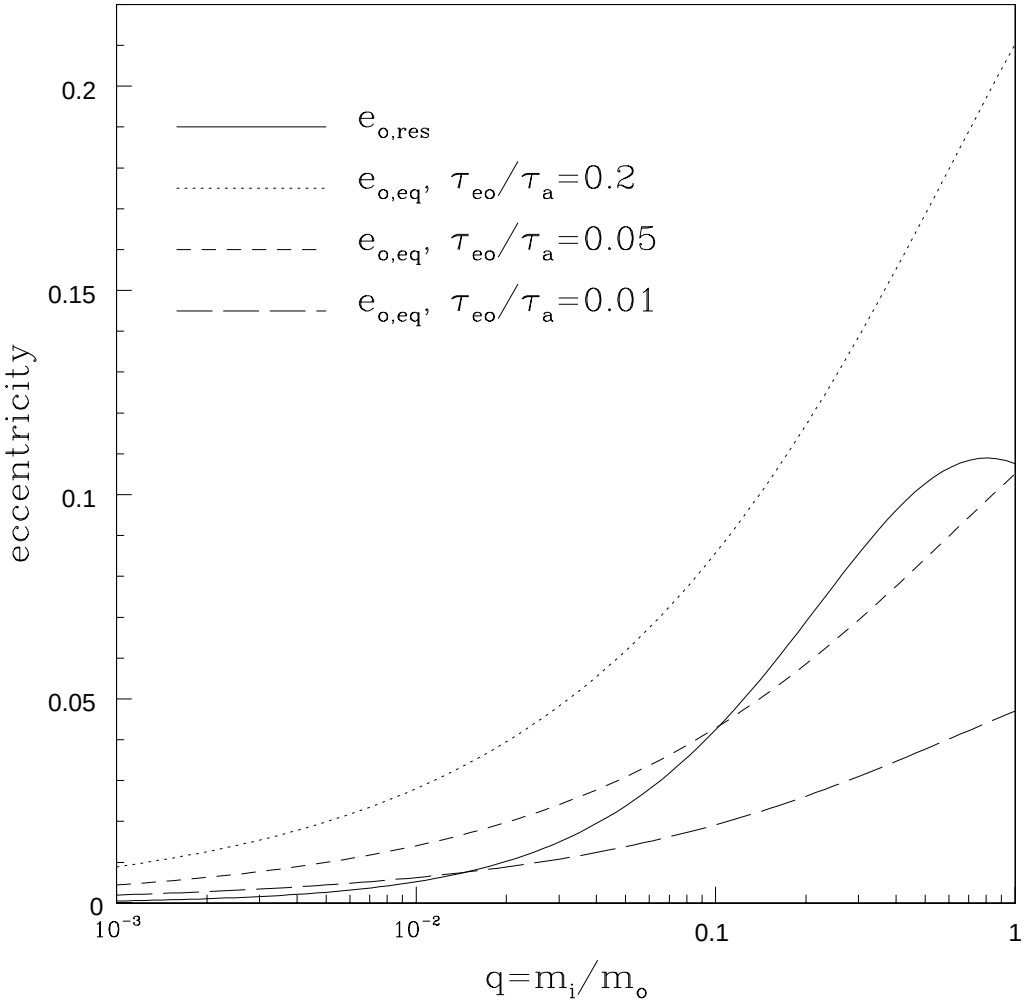

Figure 2. *Solid line:* Eccentricity $e_{\rm o,res}$ of the outer planet when the system enters an inclination–type resonance *versus* q in logarithmic scale. This curve corresponds to equation (52) with $\cos^2\phi_2 = 1$. Also shown is the equilibrium eccentricity for $\tau_{ei} \to \infty$ and $\tau_{eo}/\tau_a = 0.01$ (*long dashed line*), $\tau_{eo}/\tau_a = 0.05$ (*short dashed line*) and $\tau_{eo}/\tau_a = 0.2$ (*dotted line*). These curves correspond to equation (48). Note that the value of $e_{\rm o,res}$ found numerically for $q \lesssim 1$ is almost twice as large as that displayed here, being $\simeq 0.2$. In this context, and for $q \lesssim 1$, the system cannot enter an inclination–type resonance when $\tau_{eo}/\tau_a < 0.2$.

captured by the analysis above, as our equations are not developed up to a sufficient order in $e_{\rm i,o}$. As noted above, by expanding the perturbing function to second order in $e_{\rm i,o}$, we obtain $d\varpi_{\rm i,o}/dt$ and $d\Omega_{\rm i,o}/dt$ to zeroth order only in $e_{\rm i,o}$.

When both τ_{ei} and τ_{eo} are finite, we can find the values of q and τ_{ei}/τ_a for which inclination–type resonance may occur by writing the necessary condition $e_{\rm i,res} < e_{\rm i,eq}$. Using equations (47) and (51) and ignoring the (weak) variation of $e_{\rm i,res}$ with q, this leads to:

$$\frac{\tau_{ei}/\tau_a}{1+q\sqrt{\alpha}} > 4e_{\rm i,res}^2. \tag{53}$$

Note that the above condition is necessary but not sufficient, as we have not taken into account the fact that $e_{\rm o}$ must also reach $e_{\rm o,res}$ (we cannot write this condition as we have not calculated $e_{\rm o,eq}$ when τ_{ei} is finite). Figure 1 shows that the system cannot enter an inclination–type resonance when $\tau_{ei}/\tau_a < 0.2$. When q decreases, the inclination–type resonance is reached for shorter eccentricity damping timescales. This is expected as eccentricity is pumped up to higher values when q is smaller. We will discuss condition (53) in more details in the next section, after deriving $e_{\rm i,res}$ from the numerical simulations.

When $\tau_{ei} \to \infty$, a necessary condition for the system to enter an inclination–type resonance is $e_{\rm o,res} < e_{\rm o,eq}$. As can be seen from figure 2, and if we adopt for $q \lesssim 1$ the value of $e_{\rm o,res} \simeq 0.2$ found numerically, which is about twice as large as the value derived analytically, we find that the system cannot enter an inclination–type resonance when $\tau_{eo}/\tau_a < 0.2$.

3 NUMERICAL SIMULATIONS

The analysis presented above is valid only for small eccentricities. We now perform numerical simulations of a pair of migrating planets in the vicinity of a 2:1 mean motion resonance to extend the study to arbitrarily high eccentricities.

3.1 Equations of motion

We consider a system consisting of a primary star and two planets initially embedded in a gaseous disc surrounding the star. The planets undergo gravitational interaction with each other and the star and are acted on by tidal torques from the disc. To study the evolution of the system, we use the N–body code described in Papaloizou & Terquem (2001) in which we have added the effect of the disc torques (see also Terquem & Papaloizou 2007).

The equations of motion for the inner and outer planets are:

$$\frac{\mathrm{d}^2\mathbf{r}_\mathrm{i}}{\mathrm{d}t^2} = -\frac{Gm_\star\mathbf{r}_\mathrm{i}}{|\mathbf{r}_\mathrm{i}|^3} - \frac{Gm_\mathrm{o}(\mathbf{r}_\mathrm{i}-\mathbf{r}_\mathrm{o})}{|\mathbf{r}_\mathrm{i}-\mathbf{r}_\mathrm{o}|^3} - \sum_{\gamma=\mathrm{i,o}}\frac{Gm_\gamma\mathbf{r}_\gamma}{|\mathbf{r}_\gamma|^3} + \mathbf{\Gamma}_\mathrm{d,i} + \mathbf{\Gamma}_\mathrm{GR,i}, \tag{54}$$

$$\frac{\mathrm{d}^2\mathbf{r}_\mathrm{o}}{\mathrm{d}t^2} = -\frac{Gm_\star\mathbf{r}_\mathrm{o}}{|\mathbf{r}_\mathrm{o}|^3} - \frac{Gm_\mathrm{i}(\mathbf{r}_\mathrm{o}-\mathbf{r}_\mathrm{i})}{|\mathbf{r}_\mathrm{o}-\mathbf{r}_\mathrm{i}|^3} - \sum_{\gamma=\mathrm{i,o}}\frac{Gm_\gamma\mathbf{r}_\gamma}{|\mathbf{r}_\gamma|^3} + \mathbf{\Gamma}_\mathrm{d,o} + \mathbf{\Gamma}_\mathrm{GR,o}, \tag{55}$$

where $\mathbf{r}_\mathrm{i}$ and $\mathbf{r}_\mathrm{o}$ denote the position vector of the inner and outer planets, respectively, and we have included the acceleration of the coordinate system based on the central star (third term on the right–hand side). Acceleration due to tidal interaction with the disc is dealt with through the addition of extra forces as in Papaloizou & Larwood (2000) (see also Terquem & Papaloizou 2007):

$$\mathbf{\Gamma}_\mathrm{d,i} = -\frac{2}{t_{ei}|\mathbf{r}_\mathrm{i}|^2}\left(\frac{\mathrm{d}\mathbf{r}_\mathrm{i}}{\mathrm{d}t}\cdot\mathbf{r}_\mathrm{i}\right)\mathbf{r}_\mathrm{i}, \tag{56}$$

$$\mathbf{\Gamma}_\mathrm{d,o} = -\frac{2}{t_{eo}|\mathbf{r}_\mathrm{o}|^2}\left(\frac{\mathrm{d}\mathbf{r}_\mathrm{o}}{\mathrm{d}t}\cdot\mathbf{r}_\mathrm{o}\right)\mathbf{r}_\mathrm{o} - \frac{1}{t_m}\frac{\mathrm{d}\mathbf{r}_\mathrm{o}}{\mathrm{d}t}, \tag{57}$$

where t_m, t_{eo} and t_{ei} are the timescales over which the angular momentum of the outer planet, its eccentricity and the eccentricity of the inner planet, respectively, are damped through tidal interaction with the disc. As mentioned in section 2.3, the $1/t_m$ term is applied to the outer planet only. We show in appendix B that these forces do indeed lead to exponential damping of the eccentricities and outer semimajor axis. Note however that the migration timescale t_m defined through equation (57) is equal to twice the semimajor axis damping timescale defined through equation (39). In other words, $t_m = 2t_a$, where $t_a = \tau_a T$ and T is given by equation (21). For the eccentricity damping timescales, we simply have that t_{ei} and t_{eo} defined through equations (56) and (57) are equal to $\tau_{ei}T$ and $\tau_{eo}T$, respectively, where τ_{ei} and τ_{eo} are the dimensionless damping timescales defined in section 2.3.

Relativistic effects are included through the following acceleration:

$$\mathbf{\Gamma}_\mathrm{GR,i,o} = -\frac{6G^2m_\star^2}{c^2}\frac{\mathbf{r}_\mathrm{i,o}}{|\mathbf{r}_\mathrm{i,o}|^4}, \tag{58}$$

with c being the speed of light. It is found that this term, which induces a precession of the arguments of pericenters, does not affect significantly the results. This is because the planets do not approach the star closely enough. For this reason also, tidal interaction between the planets and the star can be neglected.

The effect of inclination damping due to planet–disc interaction, which also has not been included here, will be discussed in section 3.8 below.

3.2 Initial setting

In all the runs presented below, unless mentioned otherwise, we consider a one Jupiter mass outer planet ($m_\mathrm{o} = 1$ M$_\mathrm{J}$) and start the two planets slightly outside a 2:1 MMR at $a_\mathrm{i0} = 3.05$ AU and $a_\mathrm{o0} = 5$ AU, corresponding to a period ratio of 2.1. The initial eccentricities and inclinations are small: $e_\mathrm{i0} = e_\mathrm{o0} = 5\times10^{-3}$, $I_\mathrm{i0} = 0.01^\circ$ and $I_\mathrm{o0} = 0.02^\circ$. The longitudes of pericenters and of ascending nodes are all equal to 0° initially. We fix $t_m = 1.4\times10^6$ years which corresponds to a semimajor axis damping timescale $t_a = 7\times10^5$ years. This is roughly equal to the disc evolution timescale at 3 AU, as should be the case for type II migration. To start with, we fix for simplicity $t_{ei} = t_{eo} \equiv t_e$, i.e. $\tau_{ei} = \tau_{eo} \equiv \tau_e$, and consider different values of t_e ranging from $\sim 10^5$ to $\sim 10^6$ years. In section 3.7, we will consider $t_{ei} \to \infty$ and finite values of t_{eo}. The dependence of our results on the choice of initial conditions will be discussed in section 3.6.

3.3 Illustrative cases

In this section, we illustrate the main features of the dynamical evolution of two planets migrating in 2:1 mean motion resonance as a function of the damping eccentricity timescale. We consider strong, moderate and weak eccentricity damping,

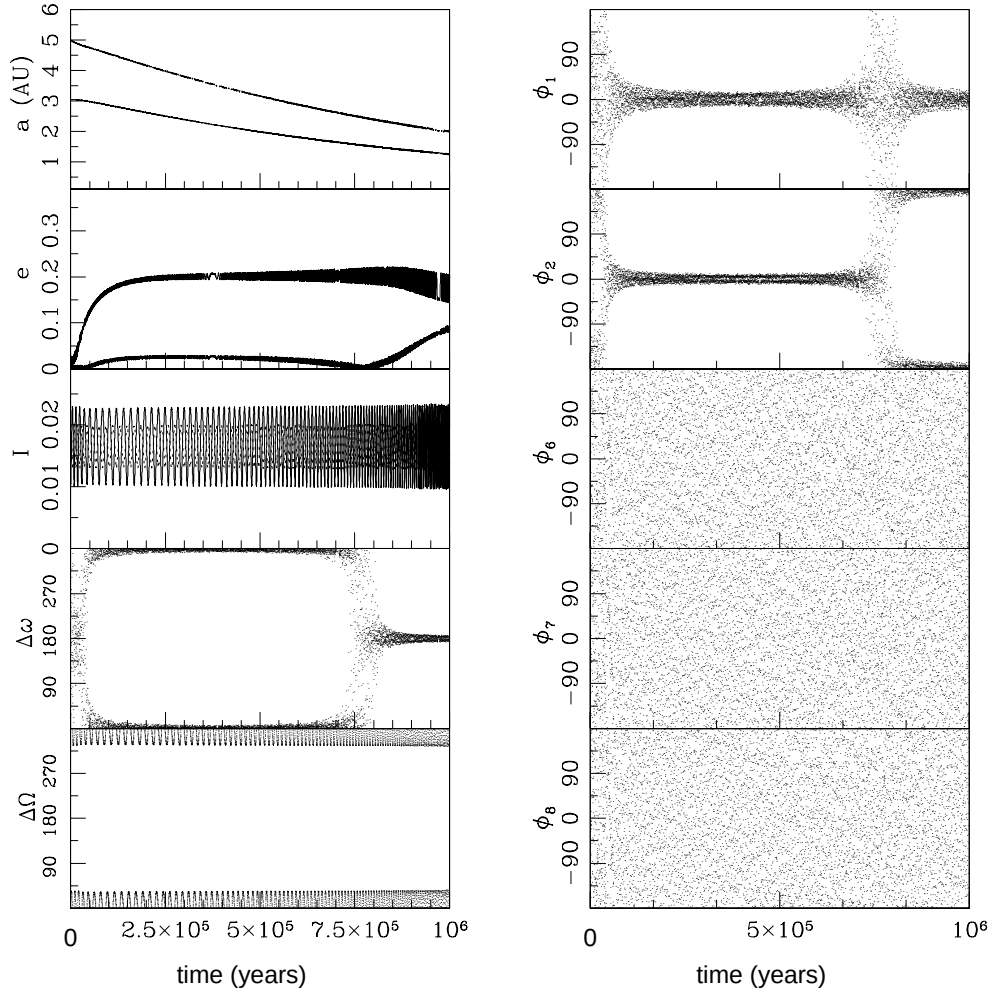

Figure 3. Evolution of a system in 2:1 mean motion resonance for $q = 0.7$ and $\tau_e/\tau_a = 0.25$ in the case $\tau_{ei} = \tau_{eo} \equiv \tau_e$. *Left column, from top to bottom:* Semi–major axes (in AU), eccentricities and inclinations of the two planets, $\Delta\varpi = \varpi_{\rm i} - \varpi_{\rm o}$ and $\Delta\Omega = \Omega_{\rm i} - \Omega_{\rm o}$ *versus* time (in years). *Right column, from top to bottom:* resonant angles ϕ_1, ϕ_2, ϕ_6, ϕ_7 and ϕ_8 *versus* time (in years). All the angles are given in degrees. In the plot displaying the eccentricities, the upper and lower curves represent $e_{\rm i}$ and $e_{\rm o}$, respectively. Shortly after the beginning of the simulation, the planets are captured into an eccentricity–type resonance: $e_{\rm i}$ grows until it reaches $e_{\rm i,eq} = 0.2$ and $\Delta\varpi$, ϕ_1 and ϕ_2 librate about 0°. After $t \simeq 8 \times 10^5$ years, $e_{\rm i}$ starts decreasing while $e_{\rm o}$ gets larger, and the value about which ϕ_2 librates switches rather abruptly to 180°. Throughout the evolution, $e_{\rm i}$ stays too small to allow for inclination–type resonance. Accordingly, the inclinations remain small, the resonant angles ϕ_6, ϕ_7 and ϕ_8 behave chaotically and $\Delta\Omega = 0$ throughout the evolution.

corresponding to $t_e/t_a \equiv \tau_e/\tau_a = 0.25$, 0.8 and 4, respectively. Here the inner planet has a mass $m_{\rm i} = 0.7$ $\rm M_J$, so that the mass ratio is $q = 0.7$.

3.3.1 Strong eccentricity damping: No inclination–type resonance

We first consider the case $t_e = 1.75 \times 10^5$ years, corresponding to $\tau_e/\tau_a = 0.25$. Figure 3 shows the evolution of $a_{\rm i,o}$, $e_{\rm i,o}$, $I_{\rm i,o}$, $\Delta\varpi = \varpi_{\rm i} - \varpi_{\rm o}$, $\Delta\Omega = \Omega_{\rm i} - \Omega_{\rm o}$, ϕ_1, ϕ_2, ϕ_6, ϕ_7 and ϕ_8 between 0 and 10^6 years. Very quickly after the beginning of the simulation, the planets capture each other in a 2:1 eccentricity–type resonance. From equation (47), we expect the eccentricity of the inner planet to reach an equilibrium value $e_{\rm i,eq} = 0.2$, in good agreement with the value observed in the simulation. At first, the resonant angles ϕ_1 and ϕ_2 librate about 0°. However, after about 8×10^5 years, as the planets get closer to each other during their convergent migration, $e_{\rm o}$ starts to increase significantly while $e_{\rm i}$ decreases, and the value about which ϕ_2 librates switches rather abruptly to 180°, which is indicative of a regime with smaller eccentricities. As expected from the analysis, $e_{\rm i}$ does not become large enough for an inclination–type resonance to develop. Accordingly, the inclinations remain small and the resonant angles ϕ_6, ϕ_7 and ϕ_8, associated with inclination–type resonances, behave chaotically.

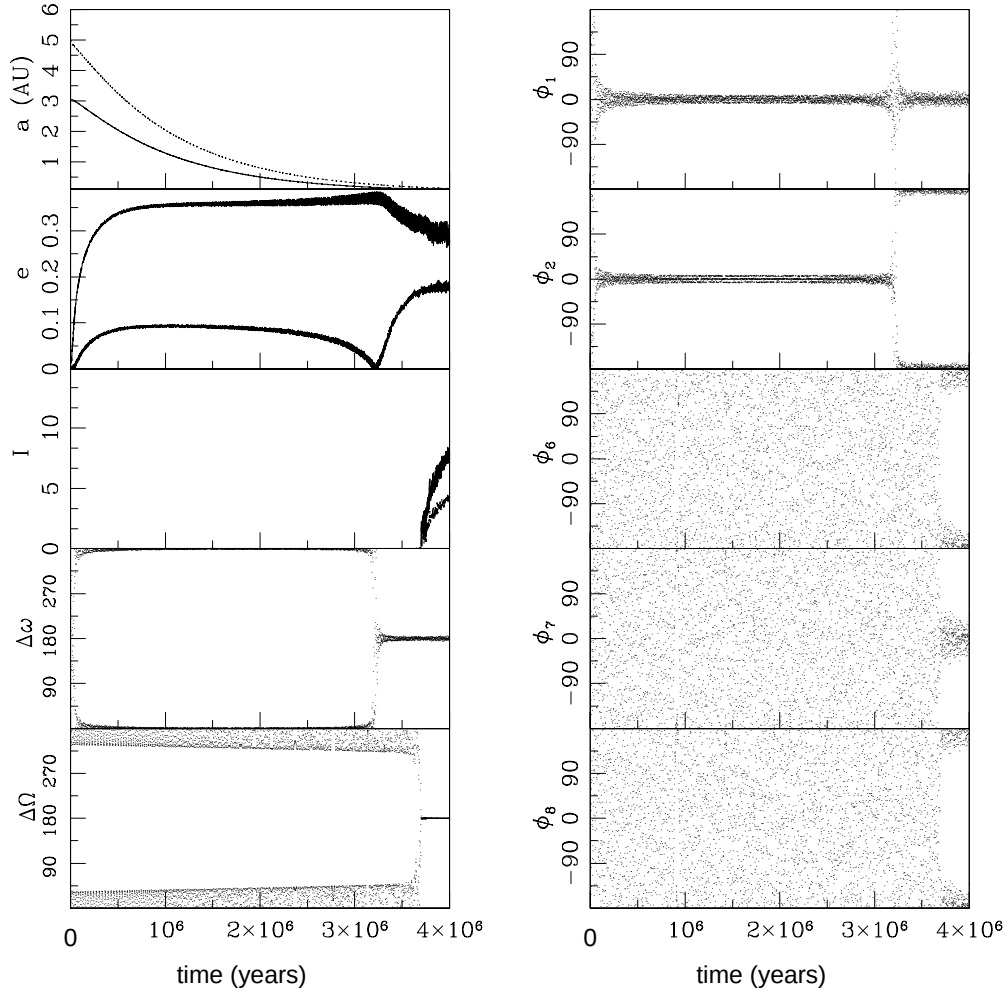

Figure 4. Same as figure 3 but for $\tau_e/\tau_a = 0.8$. In the plots displaying the eccentricities and inclinations, the upper curves represent e_i and I_i, respectively, whereas the lower curves represent e_o and I_o, respectively. Here again, shortly after the beginning of the simulation, the planets are captured into an eccentricity–type resonance: e_i grows until it reaches $e_{\mathrm{i,eq}} = 0.35$ and $\Delta\varpi$, ϕ_1 and ϕ_2 librate about 0°. After $t \simeq 3.2 \times 10^6$ years, e_i starts decreasing while e_o gets larger, and the value about which ϕ_2 librates switches to 180°. When $e_\mathrm{i} \simeq 0.3$, an inclination–type resonance starts to develop. Accordingly, the resonant angles ϕ_6, ϕ_7 and ϕ_8 start librating about 180°, 0° and 180°, respectively, while $\Delta\Omega$ librates about 180°. The inclinations grow quickly.

3.3.2 Moderate eccentricity damping: Inclination–type resonance with small eccentricities

We now consider the case $t_e = 5.6 \times 10^5$ years, corresponding to $\tau_e/\tau_a = 0.8$. The evolution of $a_\mathrm{i,o}$, $e_\mathrm{i,o}$, $I_\mathrm{i,o}$, $\Delta\varpi$, $\Delta\Omega$ and the resonant angles between 0 and 4×10^6 years are displayed in figure 4. In this case, equation (47) predicts that the eccentricity of the inner planet should reach an equilibrium value $e_{\mathrm{i,eq}} = 0.35$, in good agreement with the numerical result. We see that, at first, e_i grows very quickly, until it reaches the equilibrium value. At the same time, ϕ_1 and ϕ_2 librate about 0°. Like in the previous case, after a certain time (here $t \simeq 3.2 \times 10^6$ years), e_i starts decreasing while e_o gets larger, and the value about which ϕ_2 librates switches to 180°. When $e_\mathrm{i} \simeq 0.3$, an inclination–type resonance starts to develop, in very good agreement with the expectation from equation (51). Accordingly, the resonant angles ϕ_6, ϕ_7 and ϕ_8 start librating about 180°, 0° and 180°, respectively, while $\Delta\Omega$ librates about 180°. The inclinations grow quickly, maintaining a ratio in agreement with equation (50). The inclination–type resonance is triggered when $e_\mathrm{o} \simeq 0.18$, which is a bit larger than the value of 0.1 predicted by equation (52).

Note that, in this particular case, the inclination–type resonance occurs at $t \sim 3.5 \times 10^6$ yr, which is likely to be longer than the disc's lifetime.

We observe that the system does not enter an inclination–type resonance when e_i first reaches 0.3, at about $t = 2 \times$

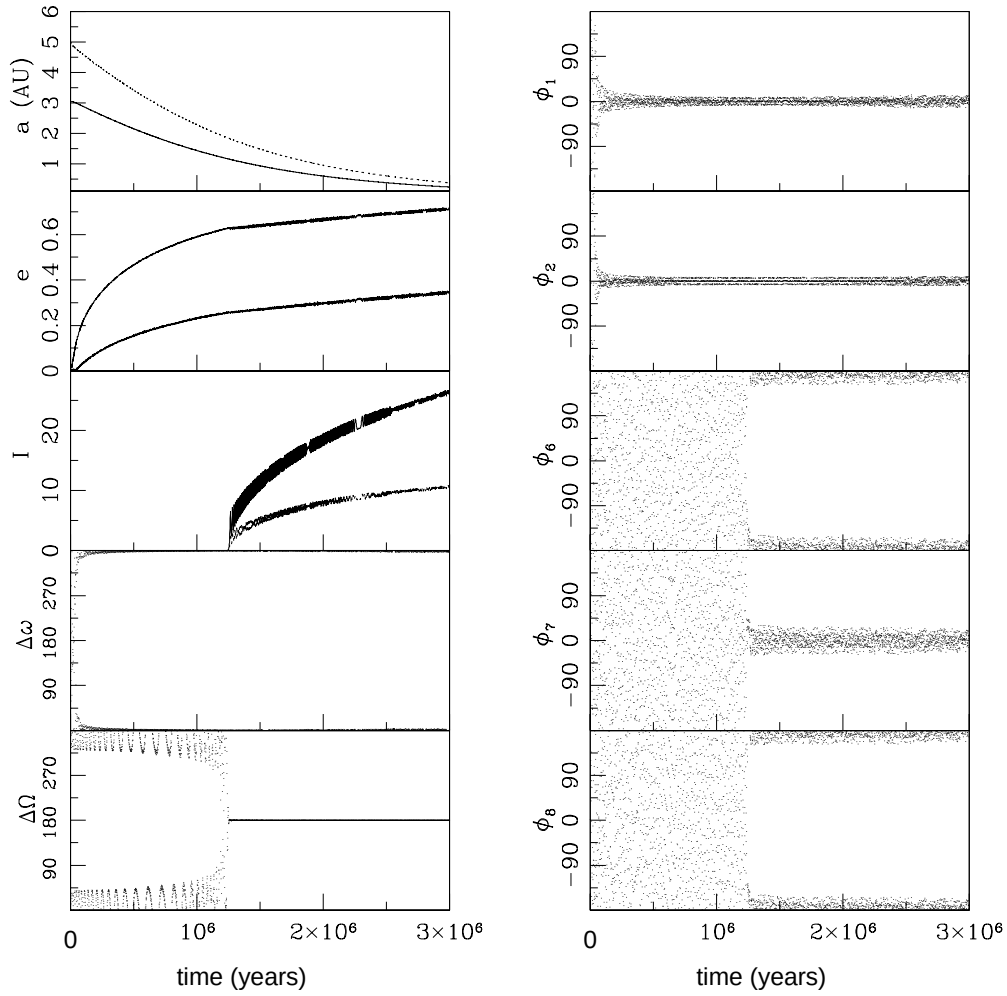

Figure 5. Same as figure 3 but for $\tau_e/\tau_a = 4$. In the plots displaying the eccentricities and inclinations, the upper curves represent e_i and I_i, respectively, whereas the lower curves represent e_o and I_o, respectively. Here again, shortly after the beginning of the simulation, the planets are captured into an eccentricity–type resonance and e_i and e_o grow. In the present case, ϕ_1 and ϕ_2 librate about 0° throughout the simulation. When $e_\mathrm{i} \sim 0.6$, the system enters an inclination–type resonance and $\Delta\Omega$, ϕ_6, ϕ_7 and ϕ_8 start librating about 180°, 180°, 0° and 180°, respectively, while the inclinations start growing.

10^5 years. This is because at that point e_o is still smaller than $e_\mathrm{o,res}$. For $q < 1$, e_o can reach $e_\mathrm{o,res}$ only when the two planets get close enough during their convergent migration for the perturbation onto the outer planet to become significant.

3.3.3 Weak eccentricity damping: Inclination–type resonance with large eccentricities

We finally consider the case $t_e = 2.8 \times 10^6$ years, corresponding to $\tau_e/\tau_a = 4$. The evolution of $a_\mathrm{i,o}$, $e_\mathrm{i,o}$, $I_\mathrm{i,o}$, $\Delta\varpi$, $\Delta\Omega$ and the resonant angles between 0 and 3×10^6 years are displayed in figure 5. In this case, equation (47) predicts that the eccentricity of the inner planet should reach an equilibrium value $e_\mathrm{i,eq} = 0.8$. As this is very large, the analysis presented in section 2.4 is probably not valid. In any case, equilibrium is not attained during the time of the simulation. Here, ϕ_1 and ϕ_2 librate about 0° throughout the simulation, which is expected for a regime with high eccentricities. Both e_i and e_o grow from the beginning of the simulation. When $e_\mathrm{i} \simeq 0.6$, at $t \simeq 1.2 \times 10^6$ years, the system enters an inclination–type resonance, characterized by $\Delta\Omega$, ϕ_6, ϕ_7 and ϕ_8 librating about 180°, 180°, 0° and 180°, respectively. This case is similar to those investigated by Thommes & Lissauer (2003).

We observe that the system does not enter an inclination–type resonance when e_i reaches 0.3 at about $t = 2 \times 10^5$ years, as e_o is still smaller than $e_\mathrm{o,res}$ at that time.

In the simulation reported here, the inclination of the outer planet stays smaller than the disc aspect ratio, so that

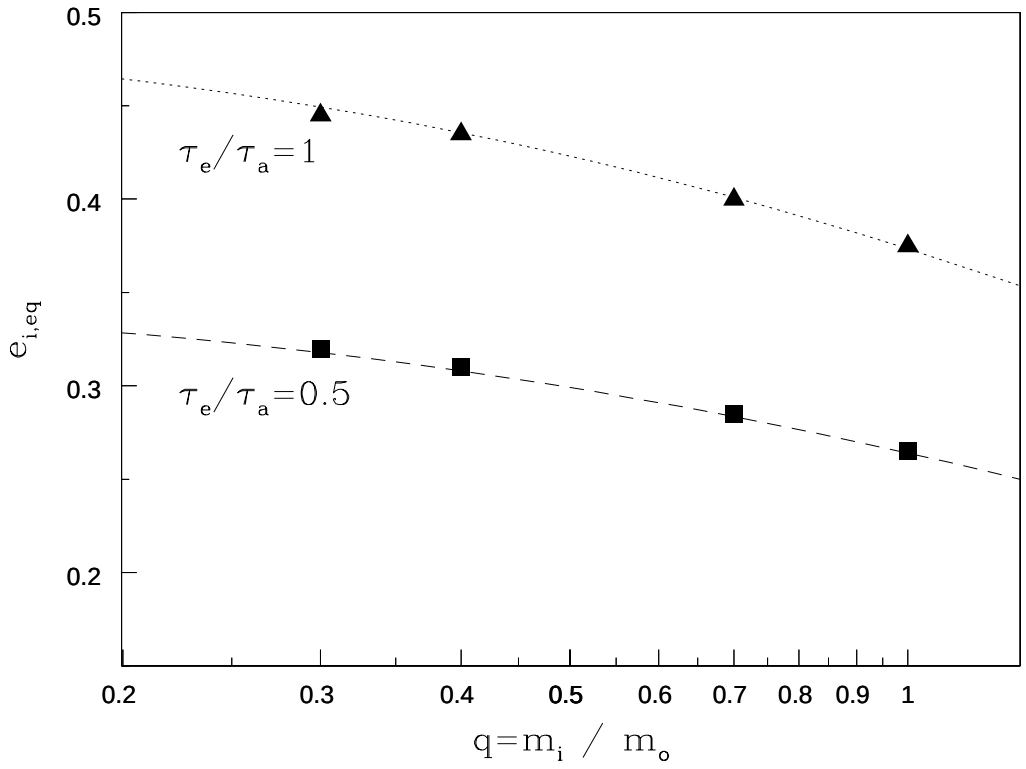

Figure 6. Equilibrium eccentricity of the inner planet *versus* mass ratio q for $\tau_e/\tau_a = 1$ *(dotted line, triangles)*, and $\tau_e/\tau_a = 0.5$ *(dashed line, squares)* in the case $\tau_{ei} = \tau_{eo} \equiv \tau_e$. The lines represent $e_{\rm i,eq}$, calculated using eq. (47) whereas the symbols represent the numerical values.

migration is not interrupted. However, we expect the inclination to become larger at some later time, so that the outer planet loses contact with the disc and stops migrating.

3.4 Comparison with analytical results

In this section, we compare the numerical values of $e_{\rm i,eq}$, $e_{\rm i,res}$, $e_{\rm o,res}$ and of the ratio $s_{\rm o}/s_{\rm i}$ when the system is in an inclination–type resonance, with the analytical values given by equations (47), (51), (52) and (50), respectively.

3.4.1 Equilibrium eccentricity of the inner planet

In section 2.4, we derived an analytical expression for the equilibrium value of $e_{\rm i}$ assuming $e_{\rm o}$ to be negligible compared to $e_{\rm i}$. As can be seen from figures 3, 4 and 5, this approximation is at least marginally valid.

In figure 6, we compare the analytical value of $e_{\rm i,eq}$ given by equation (47) with the results of the numerical integration. We consider two eccentricity damping timescales, corresponding to $\tau_e/\tau_a = 0.5$ and 1, and different values of q ranging from 0.2 to 1. We obtain very good agreement between numerical and analytical results for these values of τ_e/τ_a, even for rather large values of $e_{\rm i,eq} \sim 0.5$.

Equation (47) cannot be used for larger values of τ_e/τ_a as it would then give values of $e_{\rm i}$ too high for the second order analysis to be valid. Anyway, as will be discussed below, larger values of τ_e/τ_a are not realistic in the context of planets migrating in discs.

3.4.2 Eccentricities of the planets when the system enters an inclination–type resonance

In the analysis conducted in section 2.4, we found that inclination–type resonance would occur for $e_{\rm i} \equiv e_{\rm i,res} \sim 0.3$ (eq. [51] and fig. 1). As we have already noted, our analysis, which gives the rate of change of $\varpi_{\rm i,o}$ and $\Omega_{\rm i,o}$ only to zeroth–order in $e_{\rm i,o}$, is not valid in the regime of large eccentricities. The numerical simulations presented here do indeed confirm that there is a low eccentricity regime with $e_{\rm i,res} \simeq 0.3$, which corresponds to ϕ_1 and ϕ_2 librating about 0° and 180°, respectively. In

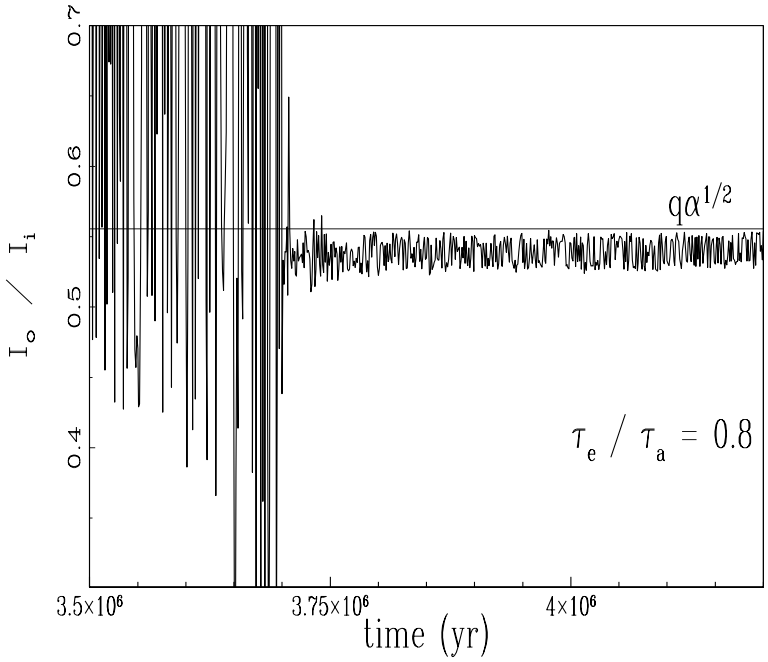

Figure 7. I_o/I_i *versus* time (in years) for $q = 0.7$ and $\tau_e/\tau_a = 0.8$ in the case $\tau_{ei} = \tau_{eo} \equiv \tau_e$. At $t \simeq 3.7 \times 10^6$ yr, the system enters an inclination–type resonance. The horizontal line represents $q\sqrt{\alpha}$, which is the value of I_o/I_i expected from the analysis. There is a reasonably good agreement between the numerical and analytical results.

addition, they show that there is a large eccentricity regime with $e_{i,res} \simeq 0.6$, which corresponds to ϕ_1 and ϕ_2 both librating about 0°.

The analysis also predicted that inclination–type resonance would occur for $e_o \equiv e_{o,res} \simeq 0.1$ for $q = 0.7$ (eq. [52]). This value should not be used in the regime $\phi_2 = 0$, as in that case e_i is large when the resonance is triggered and the equations are therefore not developped up to sufficient order in the eccentricities. In the low eccentricity regime, the value found numerically for $e_{o,res}$, 0.18, is almost twice as large as the value derived analytically. In the large eccentricity regime, the simulations give a similar value of $e_{o,res} \sim 0.2$.

3.4.3 Evolution of the inclinations

After the system enters an inclination–type resonance, according to equation (50), the inclinations evolve while maintaining a constant ratio $I_o/I_i = q\sqrt{\alpha}$ (where we have used $s_{i,o} \simeq I_{i,o}/2$, valid for small inclinations).

Numerically, we find this relation to be reasonably well satisfied. This is illustrated for $\tau_e/\tau_a = 0.8$ and $q = 0.7$ in figure 7, which shows the evolution of I_o/I_i after the system has entered an inclination–type resonance. We have also verified that the ratio of the inclinations is essentially independent of τ_a and τ_e for the values of τ_e/τ_a for which the analysis is valid.

3.5 Conditions for the onset of inclination–type resonance

In section 2.4, we derived a necessary condition (eq. [53]) for the system to enter an inclination–type resonance, which can be written as $\tau_e/\tau_a > 4e_{i,res}^2\,(1 + q\sqrt{\alpha})$. With $e_{i,res} = 0.3$, the right–hand side of this inequality varies between 0.35 and 0.65 as q varies between 0 and 1, whereas it varies between 1.4 and 2.6 for $e_{i,res} = 0.6$. We now investigate whether this condition agrees with numerical results.

We performed a series of runs with q =0.2, 0.3, 0.4, 0.7, 1 and 2 and τ_e/τ_a =0.2, 0.4, 0.5, 0.6, 0.7, 0.8, 1, 1.4, 2, 2.4, 4, 10 and 20. We integrated the equations for up to $t = 6 \times 10^6$ years, which is longer than or comparable to the age of the disc. For each run, we indicate in figure 8 whether the system entered an inclination–type resonance or not. Crosses represent runs in which there was no inclination–type resonance, open and filled symbols represent runs in which there was an inclination–type resonance with $(\phi_1, \phi_2) = (0^\circ, 180^\circ)$ or $(\phi_1, \phi_2) = (0^\circ, 0^\circ)$, respectively. Circles and triangles represent systems that entered an inclination–type resonance before or after $t = 3 \times 10^6$ years, respectively.

On this diagram, the lower dashed line is the curve $\tau_e/\tau_a = 4e_{i,res}^2\,(1 + q\sqrt{\alpha})$ (analytical condition [53]) with $e_{i,res} = 0.3$. For $q \leq 0.7$, this curve approximates very well the boundary between systems which do not enter an inclination–type resonance and systems which do enter such a resonance with $(\phi_1, \phi_2) = (0^\circ, 180^\circ)$, i.e. while maintaining small eccentricities. These results

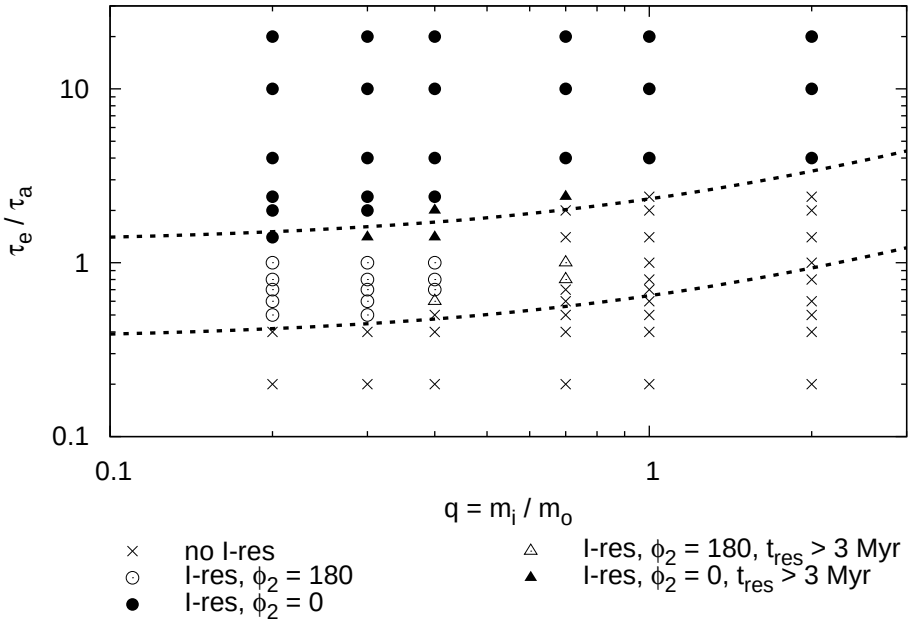

Figure 8. Occurrence of inclination–type resonance as a function of q and τ_e/τ_a in systems evolved between 0 and 6 Myr. Here $\tau_{ei} = \tau_{eo} \equiv \tau_e$. *Crosses* represent systems that did not enter an inclination–type resonance, *open* and *filled symbols* represent systems that entered an inclination–type resonance with $(\phi_1, \phi_2) = (0°, 180°)$ or $(\phi_1, \phi_2) = (0°, 0°)$, respectively. *Circles* and *triangles* represent systems that entered an inclination–type resonance before or after $t = 3$ Myr, respectively. The *dashed lines* are the curves $\tau_e/\tau_a = 4e_{\rm i,res}^2\left(1 + q\sqrt{\alpha}\right)$ with $e_{\rm i,res} = 0.3$ (*lower line*) and $e_{\rm i,res} = 0.57$ (*upper line*). In agreement with theoretical expectations, systems in between those two lines entered an inclination–type resonance with $(\phi_1, \phi_2) = (0°, 180°)$ if evolved long enough, whereas systems above the upper line entered an inclination–type resonance with $(\phi_1, \phi_2) = (0°, 0°)$.

confirm the analytical result $e_{\rm i,res} \simeq 0.3$ (eq. [51] and fig. 1). We note that, as q gets larger (heavier inner planet), it takes longer for an inclination–type resonance to be excited, which is consistent with the fact that it takes longer for the eccentricity of the inner planet to grow. This probably explains why systems above the dashed curve have not entered an inclination–type resonance for the largest values of q. We would expect these systems to enter such a resonance if we carried on the integration beyond 6 Myr.

The upper dashed line is the curve $\tau_e/\tau_a = 4e_{\rm i,res}^2\left(1 + q\sqrt{\alpha}\right)$ (analytical condition [53]) with $e_{\rm i,res} = 0.57$, value which gives the best fit to the boundary between runs which enter an inclination–type resonance for $(\phi_1, \phi_2) = (0°, 180°)$ and those which enter the resonance for $(\phi_1, \phi_2) = (0°, 0°)$. The fact that this boundary can be fitted with this curve indicates that the analysis leading to the expression (47) of the equilibrium value of $e_{\rm i}$ (which is used in deriving eq. [53]) is still valid in the regime of rather large eccentricities, as already noted in section 3.4.1, and also that $e_{\rm i,res}$ is essentially independent of q and τ_e/τ_a in the large eccentricity regime (see also Thommes & Lissauer 2003).

3.6 Influence of varying t_a and $m_{\rm o}$

In the simulations presented above, we fixed $m_{\rm o} = 1$ M$_{\rm J}$ and $t_a = 7 \times 10^5$ years (consistent with type II migration timescale at a few AU from the star). Then $q \equiv m_{\rm i}/m_{\rm o}$ and $\tau_e/\tau_a \equiv t_e/t_a$ were varied. We have checked that the results reported above are unaffected if we take t_a to be 5×10^5 or 10^6 years and $m_{\rm o}$ to be 0.5 M$_{\rm J}$.

The *Kepler* mission has found planets with a mass comparable to or lower than that of Neptune to be very common. Figure 9 shows the evolution of two Neptune mass planets ($m_{\rm o} = m_{\rm i} = 0.05$ M$_{\rm J}$) with $t_a = 2 \times 10^5$ years and $\tau_e/\tau_a = 4$. As in the case of two Jupiter mass planets illustrated above, the system enters an inclination–type resonance when $e_{\rm i} \sim 0.6$.

3.7 Case where the eccentricity of the inner planet is not damped

So far, we have assumed that both planets were interacting with the disc so that both eccentricities were damped (t_{ei} and t_{eo} both finite). In this section, we consider the case where the planets evolve in a cavity, with only the outer planet maintaining contact with the disc. Eccentricity damping therefore acts only on the outer planet ($t_{ei} \to \infty$ and t_{eo} finite). This situation may arise if the planets clear–out a gap which is deep enough that the parts of the disc interior to the orbits are no longer

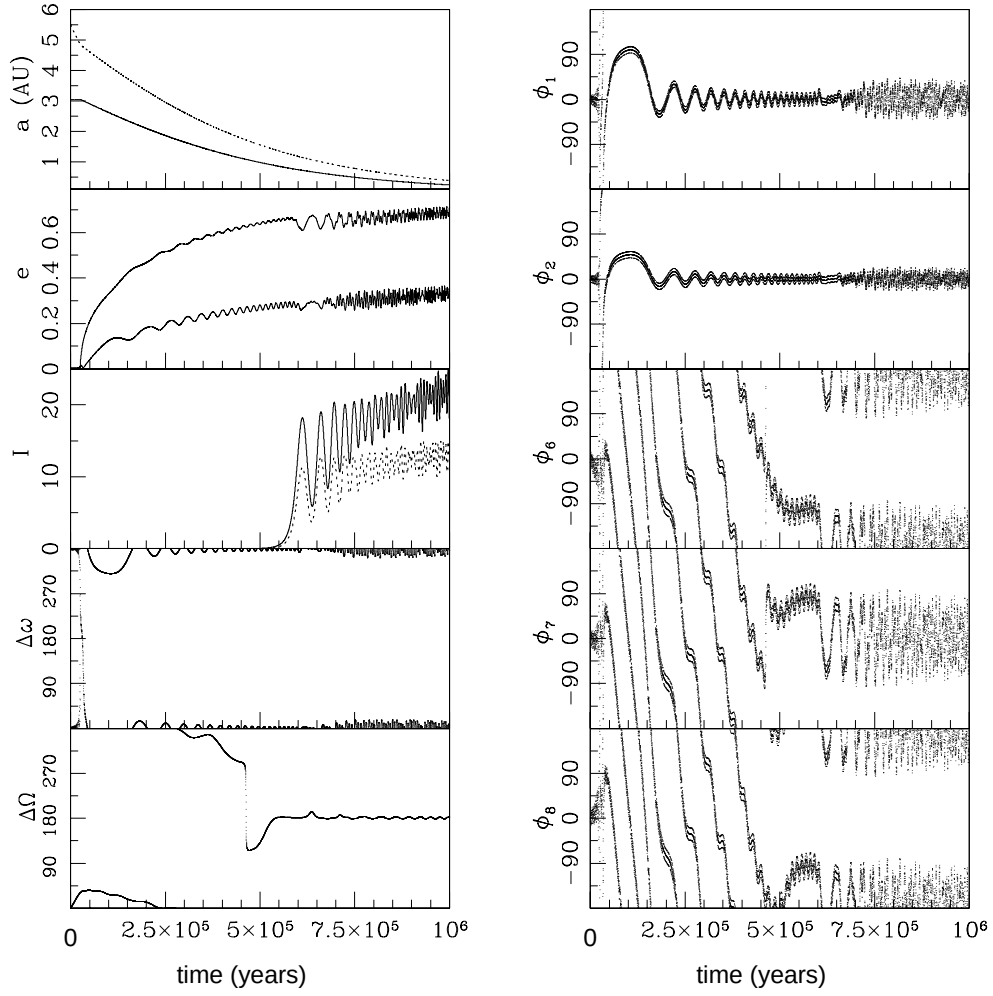

Figure 9. Same as figure 5 but for $m_{\rm o} = m_{\rm i} = 0.05$ M$_{\rm J}$ and $t_a = 2 \times 10^5$ years (and $\tau_e/\tau_a = 4$ as in fig 5). The evolution is very similar to that observed in figure 5 for two Jupiter mass planets.

replenished efficiently from the outer disc. The inner disc accretes onto the star over a viscous timescale. If the outer planet migrates in over a similar timescale, pushing in the inner planet, contact between the disc and the inner planet is maintained. However, is the outer planet migrates over a slower timescale, which happens when the mass of the planet is larger than that of the disc in the vicinity of its orbit, the inner planet loses contact with the disc. Note that, if the pair of planets enters an inner cavity carved, e.g., by photoevaporation, migration of the outer planet ceases and eccentricities cannot grow anymore, which would prevent the onset of inclination–type resonance.

We perform the same numerical simulations as above except that now $\mathbf{\Gamma}_{\rm d,i}$ in equation (54) is set to zero, whereas $\mathbf{\Gamma}_{\rm d,o}$ in equation (55) remains unchanged. Figure 10 shows the eccentricities, inclinations and resonant angle ϕ_2 for $\tau_e/\tau_a = 0.25, 0.3$ and 0.01, where $\tau_e \equiv \tau_{eo}$.

The case $\tau_e/\tau_a = 0.25$ is the same as that shown on figure 3 with a finite τ_{ei}. When $\tau_{ei} \to \infty$, the eccentricities reach much larger values. However, $e_{\rm i}$ saturates just below 0.6, which is not sufficient to trigger an inclination–type resonance with $(\phi_1, \phi_2) = (0^\circ, 0^\circ)$. Note that $e_{\rm i}$ passed through the value 0.3, which we found to be, in principle, sufficient to trigger an inclination–type resonance with $(\phi_1, \phi_2) = (0^\circ, 180^\circ)$. However, when $e_{\rm i} = 0.3$, $e_{\rm o}$ is only about 0.05, below the value $e_{\rm o,res}$ required for the resonance to be excited.

For $\tau_e/\tau_a = 0.3$, the inclination–type resonance is not excited when the eccentricity of the inner planet is damped (see figure 8). Here however, we see that $e_{\rm i}$ grows to large values and eventually reaches 0.6, at which point an inclination–type resonance with $(\phi_1, \phi_2) = (0^\circ, 0^\circ)$ is triggered. Therefore, in this case, suppressing eccentricity damping on the inner planet significantly affects the evolution of the system.

Figure 10 also shows the case $\tau_e/\tau_a = 0.01$. Damping of the outer planet eccentricity is too strong for either $e_{\rm i,res}$ or

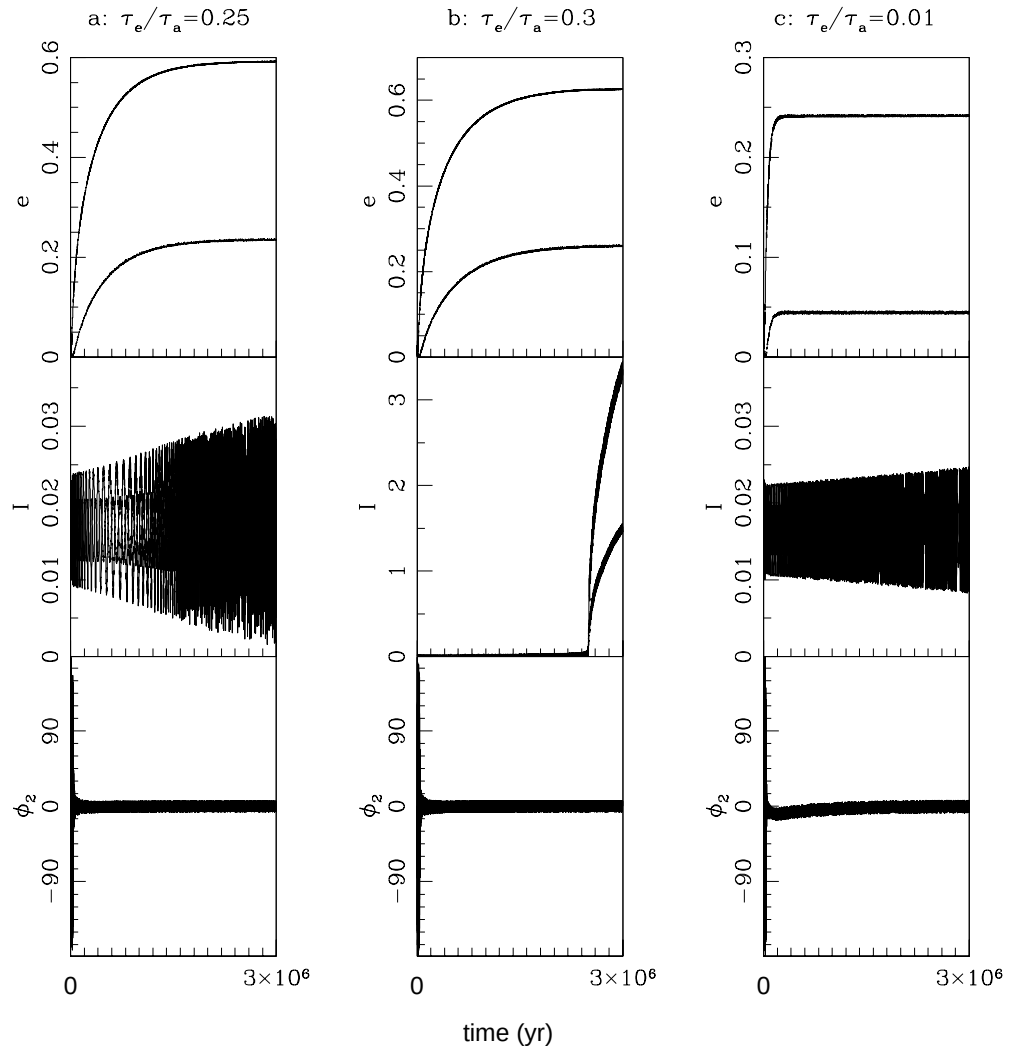

Figure 10. Evolution of a system in 2:1 mean motion resonance for $q = 0.7$ and $\tau_{ei} \to \infty$. Here $\tau_e \equiv \tau_{eo}$. *From top to bottom:* Eccentricities and inclinations (in degrees) of the two planets and resonant angle ϕ_2 (in degrees) *versus* time (in years) for $\tau_e/\tau_a = 0.25$ (*left column*), 0.3 (*middle column*) and 0.01 (*right column*). In the plots displaying the eccentricities, the upper and lower curves correspond to $e_{\rm i}$ and $e_{\rm o}$, respectively. The case with $\tau_e/\tau_a = 0.25$ is the same as that displayed on figure 3 except for τ_{ei} which is infinite here.

$e_{\rm o,res}$ to be reached. We see on figure 10 that the values at which $e_{\rm o}$ saturates agree very well with the expectation from equation (48).

The value of $e_{\rm o,res}$ we have calculated analytically is not valid in the regime $\phi_2 = 0^\circ$ which is observed here. In this regime however, numerical simulations performed for finite values of τ_{ei} and $q = 0.7$ indicate that $e_{\rm o,res} \simeq 0.2$. We see on figure 2 that $e_{\rm o}$ cannot reach this value for $\tau_e/\tau_a < 0.2$, which is in good with the fact that inclination–type resonance is observed for $\tau_e/\tau_a = 0.3$ but not for $\tau_e/\tau_a = 0.25$ or 0.01.

3.8 Effect of inclination damping

So far, we have ignored damping of the inclinations due to interaction with the disc. For the range of inclinations and eccentricities considered here, inclination and eccentricity damping are expected to occur over similar timescales (Bitsch et al. 2013 for gap opening planets, Cresswell et al. 2007 for non gap opening planets). Inclination damping can therefore be taken into account by adding the following term on the right–hand side of equations (56) and (57) (Papaloizou & Larwood 2000):

$$-\frac{2}{t_i}\left(\frac{{\rm d}\mathbf{r}_{\rm i,o}}{{\rm d}t}\cdot\mathbf{e}_z\right)\mathbf{e}_z \tag{59}$$

where $\mathbf{e}_z$ is the unit vector perpendicular to the disc midplane, and t_i the inclination damping timescale, which is of the same

order as the eccentricity damping timescale. We have run a few simulations which show that the addition of this extra force does not strongly affect the dynamics of the system. Inclination–type resonances are found to occur for the same values of the parameters as above, and are characterized by libration of the resonant angles about the same values as when there is no inclination damping.

Inclination damping has little effect because it happens over the same timescale as eccentricity damping. When t_e is small, inclination–type resonances do not occur, and therefore inclination damping is irrelevant. On the contrary, when t_e is large enough that inclination–type resonances are excited, inclination damping is too weak to affect the sudden increase of the inclinations. It would however limit the growth of the inclinations over a timescale longer than the time during which the simulations were run.

4 DISCUSSION

4.1 Summary of the main results

In this paper, we have studied analytically the evolution of the eccentricities of a pair of planets locked in a 2:1 mean motion resonance. In the early stages of the evolution, the planets are in an eccentricity–type resonance, in which the orbits are in the plane of the disc. We have derived the equilibrium eccentricity $e_{\rm i,eq}$ reached by the inner planet after a time large compared to the eccentricity damping timescale (eq. [47]) in the case where the eccentricities of both planets are damped. In the case where only the eccentricity of the outer planet is damped, we have calculated its equilibrium value $e_{\rm o,eq}$ (eq. [48]).

We have shown that, for the system to enter an inclination–type resonance, the eccentricity of the inner planet has to reach a value $e_{\rm i,res} \sim 0.3$, independent of the migration and eccentricity damping timescales and only weakly dependent on the mass ratio q for $q \leq 1$ (eq. [51] and fig. 1). Numerically, we have also shown that there is another, larger, value of $e_{\rm i,res} \simeq 0.6$ (which was found by Thommes & Lissauer 2003). When the system enters an inclination–type resonance with $e_{\rm i,res} \simeq 0.3$ (*small eccentricity* regime), the resonant angles ϕ_1 and ϕ_2 librate about 0° and 180°, respectively. In the *large eccentricity* regime ($e_{\rm i,res} \simeq 0.6$), ϕ_1 and ϕ_2 both librate about 0°.

We have also derived analytically the value $e_{\rm o,res}$ that the eccentricity of the outer planet has to reach for an inclination–type resonance to be excited. In the low eccentricity regime, we find $e_{\rm o,res} \simeq 0.1$ for a mass ratio $q \lesssim 1$. This value is somewhat smaller than that found numerically, which is $\simeq 0.2$. In the large eccentricity regime, the numerical simulations also give $e_{\rm o,res} \simeq 0.2$ for $q \lesssim 1$.

If $e_{\rm i}$ reaches $e_{\rm i,eq}$ while $e_{\rm o}$ is still below $e_{\rm o,eq}$, the system keeps evolving in the eccentricity–type resonance. As the planets approach each other during their convergent migration, $e_{\rm o}$ increases and may at some point reach $e_{\rm o,eq}$. The system may then enter an inclination–type resonance with either $e_{\rm i} \simeq 0.3$ or $\simeq 0.6$ if the eccentricity of the inner planet has continued to increase.

Necessary conditions for the system to enter an inclination–type resonance are $e_{\rm i,res} < e_{\rm i,eq}$ and $e_{\rm o,res} < e_{\rm o,eq}$. This leads to a condition on the ratio of the eccentricity damping timescale to the semimajor axis damping timescale, t_e/t_a, as a function of the mass ratio $q = m_{\rm i}/m_{\rm o}$ (eq.[53] and fig. 1 for the case where both eccentricities are damped and fig. 2 for the case where only the eccentricity of the outer planet is damped). *For $q \leq 1$ and when both eccentricities are damped, we find that the system cannot enter an inclination–type resonance if $t_e/t_a < 0.2$. This result still holds when only the eccentricity of the outer planet is damped, at least for $q \lesssim 1$.*

4.2 Implication for extrasolar planetary systems

Whether or not the orbit of an extrasolar planet embedded in a disc and locked in a mean motion resonance with a heavier outer companion may become inclined due to an inclination–type resonance depends on whether the eccentricity of the planet can become as high as 0.3. This in turn depends (weakly) on the mass ratio q and (strongly) on t_e/t_a.

For a wide range of planet masses, the eccentricity damping timescale due to planet/disc interaction is on the order of a hundred orbits (see Papaloizou & Larwood 2000, Cresswell et al. 2007 and Bitsch & Kley 2010 for masses $\sim 1 - 10$ $\rm M_\oplus$, 20 $\rm M_\oplus$ and 0.1–1 $\rm M_J$, respectively), i.e. shorter than 10^3 years for a planet at a few AU from the central star. As type I and type II migration timescales at this location are on the order of 10^5 years, this implies that $t_e/t_a \sim 10^{-2}$, much smaller than the value needed for $e_{\rm i,res}$ to be reached.

Even when the eccentricity of the inner planet is not damped, and for $q \lesssim 1$, disc torques acting on the outer planet are still too strong for enabling its eccentricity to reach the value required for the onset of an inclination–type resonance.

Lee & Peale (2002) calculated the value of τ_e/τ_a consistent with the observed eccentricities of the two giant planets around GJ 876, which are found to be in a 2:1 mean motion resonance, assuming the system had migrated inward. They found that in the case where the semimajor axes and eccentricities of both planets were assumed to be damped, τ_e/τ_a had to be about 0.1, whereas it had to be about 0.01 in the case where only the semimajor axis and eccentricity of the outer planet

were damped. According to the results presented in this paper, in neither of these cases could an inclination–type resonance be triggered.

We conclude that the excitation of inclination through the type of resonance described here is very unlikely to happen in a system of two planets migrating in a disc. If the eccentricities of both planets are damped, this conclusion does not depend on the mass ratio of the planets. If only the eccentricity of the outer planet is damped, this conclusion holds for at least $q \lesssim 1$. This is consistent with the fact that orbits in the multiplanet systems detected by *Kepler* seem to have both low inclinations (Fabrycky et al. 2012) and low eccentricities (Kane et al. 2012). It is also therefore very unlikely that inclination–type resonance is the cause of the orbital inclination observed for a number of hot Jupiters.

ACKNOWLEDGEMENTS

We thank our anonymous referee for helpful comments and suggestions that improved the manuscript.

REFERENCES

Bate, M., Lodato, G., Pringle, J., 2010, MNRAS, 401, 1505
Batygin, K., 2012, Nature, 491, 418
Beaugé, C., Ferraz-Mello, S., Michtchenko, T., 2003, ApJ, 593, 1124
Bitsch, B., Kley, W., 2010, A&A, 523, 30
Bitsch, B., Crida A., Libert A.-S., Lega E., 2013, A&A, 555, 124
Burns, J.A, 1976, Am. J. Phys. 44. 944-949
Chatterjee, S., Ford, E., Matsumura, S., Rasio, F., 2008, ApJ, 686, 580
Cresswell, P., Dirksen, G., Kley, W., Nelson, R., 2007, A&A, 473, 329
Fabrycky, D., Tremaine, S., 2007, ApJ, 669, 1298
Fabrycky, D., et al., 2012, ApJ, 750, 114
Foucart, F., Lai, D., 2011, MNRAS, 412, 2799
Goldreich, P., 1965, MNRAS, 130, 159
Goldreich, P., Schlichting, H., 2014, Astron. J., 147, 32G
Greenberg, R., 1977, Vistas in Astronomy, 21, 209
Kane, S., Ciardi, D., Gelino, D., von Braun, K., 2012, MNRAS, 425, 757
Kley, W., Lee M., Murray N., Peale S., 2005, A&A 437, 727
Lai, D., Foucart, F., Lin, D., 2011, MNRAS, 412, 2790
Lee, M., 2004, ApJ, 611, 517
Lee, M., Peale S., 2002, ApJ, 567, 596
Lee, M., Thommes E., 2009, ApJ, 702, 1662
Libert, A.-S., Tsiganis, K., 2009, MNRAS, 400, 1373
Lissauer, J., Peale, S., Cuzzi, J., 1984, Icarus, 58, 159
Lissauer, J., et al., 2011, ApJS, 197, 8
Lissauer, J., et al., 2014, ApJ, 784, 44
Marcy, G., Butler, R., Fischer, D., Vogt, S., Lissauer, J., Rivera, E., 2001, ApJ, 556, 296
Murray, C., Dermott, S., 1999, Solar System Dynamics, Cambridge University Press
Naoz, S., Farr, W., Lithwick, Y., Rasio, F., Teyssandier, J., 2011, Nature, 473, 187
Papaloizou, J., Larwood, J., 2001, MNRAS, 315, 823
Papaloizou, J., Terquem, C., 2001, MNRAS, 325, 221
Peale, S., 1976, ARA&A, 14, 215
Petrovich, C., Malhotra, R., Tremaine, S., 2013, ApJ, 770, 24
Rowe, J., et al, 2014, ApJ, 784, 45
Roy, A. E., 1978, Orbital motion, Institute of Physics, London, 4th edition 2005, p. 212
Snellgrove, M., Papaloizou, J., Nelson, R., 2001, A&A, 374, 1092
Terquem, C., 2013, MNRAS, 435, 798
Terquem, C., Papaloizou J., 2007, ApJ, 654, 1110
Thommes, E., Lissauer, J., 2003, ApJ, 597, 566
Wu, Y., Lithwick, Y., 2011, ApJ, 735, 109
Wu, Y., Murray, N., Ramsahai, J., 2007, ApJ, 670, 820

Coefficient	Expression	Numerical value at the 2:1 resonance
f_1	$-\frac{1}{2}\left(4+\alpha\mathrm{D}\right)b_{1/2}^{(2)}$	-1.19049
f_2	$\frac{1}{2}\left(3+\alpha\mathrm{D}\right)b_{1/2}^{(1)}$	1.68831
f_2^m	$f_2-2\alpha$	0.42839
f_3	$\frac{1}{8}\left(44+14\alpha\mathrm{D}+\alpha^2\mathrm{D}^2\right)b_{1/2}^{(4)}$	1.69573
f_4	$-\frac{1}{4}\left(42+14\alpha\mathrm{D}+\alpha^2\mathrm{D}^2\right)b_{1/2}^{(3)}$	-4.96685
f_5	$\frac{1}{8}\left(38+14\alpha\mathrm{D}+\alpha^2\mathrm{D}^2\right)b_{1/2}^{(2)}$	3.59380
f_6	$\frac{1}{2}\alpha b_{3/2}^{(3)}$	0.81988
f_7	$-\alpha b_{3/2}^{(3)}$	-1.63976
f_8	$\frac{1}{2}\alpha b_{3/2}^{(3)}$	0.81988
K_1	$\frac{1}{8}\left(2\alpha\mathrm{D}+\alpha^2\mathrm{D}^2\right)b_{1/2}^{(0)}$	0.38763
K_2	$\frac{1}{4}\left(2-2\alpha\mathrm{D}-\alpha^2\mathrm{D}^2\right)b_{1/2}^{(1)}$	-0.57570
K_3	$-\frac{1}{2}\alpha b_{3/2}^{(1)}$	-1.55051
K_4	$\alpha b_{3/2}^{(1)}$	3.10102

Table A1. Expression and numerical value at the 2:1 mean motion resonance of the coefficients which enter the expression of the disturbing function

APPENDIX A: COEFFICIENTS IN THE DISTURBING FUNCTION

In table A, we give the expression of the coefficients f_i $(i=1,\ldots,8)$ and K_i $(i=1,\ldots,4)$ which enter the expression of the direct part of the disturbing function in equations (3) and (4). We denote $b_s^{(j)}(\alpha)$ the Laplace coefficient defined by:

$$b_s^{(j)}(\alpha)=\frac{1}{\pi}\int_0^{2\pi}\frac{\cos(j\psi)}{\left(1-2\alpha\cos\psi+\alpha^2\right)^s}\,\mathrm{d}\psi, \tag{A1}$$

where j is an integer and s is a half integer. We define $\mathrm{D}\equiv \mathrm{d}/\mathrm{d}\alpha$. In table A, we also give the numerical value of the f_i $(i=1,\ldots,8)$ and K_i $(i=1,\ldots,4)$ evaluated at the 2:1 mean motion resonance, where $\alpha=2^{-2/3}$.

APPENDIX B: DAMPING FORCES

In the N–body simulations performed in this paper, the damping force due to the interaction between the outer planet and the disc is given by equation (57), which we can rewrite under the form:

$$\mathbf{\Gamma}_\mathrm{d}=-\left(\frac{1}{t_m}+\frac{2}{t_e}\right)\dot{r}\;\mathbf{e}_r-\frac{1}{t_m}r\dot{\theta}\;\mathbf{e}_\theta, \tag{B1}$$

where we have dropped the subscript 'o' which we have used for the outer planet. Here r and θ are the polar coordinates referred to the central star, $\mathbf{e}_r$ and $\mathbf{e}_\theta$ are the unit vectors along and perpendicular to the radius vector $\mathbf{r}$, respectively, in the orbital plane, and the dot denotes a time–derivative.

We now show that adding this force to the equation of motion is equivalent to adding the terms $-a/t_a-2ae^2/t_e$, with $t_a=t_m/2$, in the expression of da/dt and the term $-e/t_e$ in the expression of de/dt, as done in section 2.3 (see eq. [39] and [41]).

The total energy and angular momentum vector per unit mass of the planet are $E=-Gm_\star/(2a)$ and $\mathbf{H}=r^2\dot{\theta}\mathbf{e}_z$, respectively, where $\mathbf{e}_z=\mathbf{e}_r\times\mathbf{e}_\theta$. Because the planet is acted on by the perturbative force (B1), E and $\mathbf{H}$ vary with time according to:

$$\dot{E} = \dot{\mathbf{r}} \cdot \mathbf{\Gamma}_{\rm d}, = -\left(\frac{1}{t_m} + \frac{2}{t_e}\right) \dot{r}^2 - \frac{1}{t_m}(r\dot{\theta})^2, \tag{B2}$$

$$\dot{\mathbf{H}} = \mathbf{r} \times \mathbf{\Gamma}_{\rm d}, = -\frac{1}{t_m} r^2 \dot{\theta} \mathbf{e}_z. \tag{B3}$$

The rate of change of a and e is related to that of E and H through (e.g., Burns 1976):

$$\frac{da}{dt} = \frac{2a^2}{Gm_\star}\dot{E}, \tag{B4}$$

$$\frac{de}{dt} = \frac{1}{2e}(e^2-1)\left(2\frac{\dot{H}}{H} + \frac{\dot{E}}{E}\right). \tag{B5}$$

Substituting equation (B2) into equation (B4), we obtain:

$$\left\langle \frac{da}{dt} \right\rangle = \frac{2a^2}{Gm_\star}\left[-\left(\frac{1}{t_m} + \frac{2}{t_e}\right)\left\langle \dot{r}^2 \right\rangle - \frac{1}{t_m}\left\langle (r\dot{\theta})^2 \right\rangle\right], \tag{B6}$$

where the brackets denote time–averaging over an orbital period. To perform the time–averaging, we first write $\dot{r}$ and $r\dot{\theta}$ in terms of the true anomaly f:

$$\dot{r} = \frac{na}{\sqrt{1-e^2}} e \sin f, \tag{B7}$$

$$r\dot{\theta} = \frac{na}{\sqrt{1-e^2}} (1 + e\cos f). \tag{B8}$$

We then use the expansion of $\cos f$ and $\sin f$ in terms of the mean anomaly M, which is 2π–periodic and a linear function of time. To obtain $\langle da/dt \rangle$ and $\langle de/dt \rangle$ to second–order in e, we only need to expand $\cos f$ and $\sin f$ to first–order in e. This gives:

$$\cos f = \cos M + e(\cos 2M - 1), \tag{B9}$$

$$\sin f = \sin M + e \sin 2M, \tag{B10}$$

so that $\left\langle \dot{r}^2 \right\rangle = n^2 a^2 e^2/2$ and $\left\langle (r\dot{\theta})^2 \right\rangle = n^2 a^2 (1 - e^2/2)$. Substituting into equation (B6) and using $Gm_\star = n^2 a^3$, we finally obtain:

$$\left\langle \frac{{\rm d}a}{{\rm d}t} \right\rangle = -2a\left(\frac{1}{t_m} + \frac{e^2}{t_e}\right). \tag{B11}$$

To calculate the rate of change of e, we now substitute equations (B3) and (B4) into equation (B5), and use the expression of E and H to obtain:

$$\left\langle \frac{de}{dt} \right\rangle = \frac{1}{2e}(e^2-1)\left(-\frac{2}{t_m} - \frac{1}{a}\left\langle \frac{da}{dt} \right\rangle\right). \tag{B12}$$

Substituting equation (B11), this gives:

$$\left\langle \frac{de}{dt} \right\rangle = -\frac{1}{t_e} e. \tag{B13}$$

Therefore, as anticipated, adding the damping force (B1) to the equation of motion is equivalent to adding the terms in equations (B11) and (B13) to the rate of change of a and e.